HHS Public Access

Author manuscript

Radiol Clin North Am. Author manuscript; available in PMC 2022 September 01.

Published in final edited form as:

Radiol Clin North Am. 2021 September ; 59(5): 887–918. doi:10.1016/j.rcl.2021.05.012.

Novel Tracers and Radionuclides in PET Imaging

Christian Mason, PhD[a], **Grayson R. Gimblet, BS**[b,1], **Suzanne E. Lapi, PhD**[c,d,1], **Jason S. Lewis, PhD**[a,e,f,*]

[a]Department of Radiology, Memorial Sloan Kettering Cancer Center, 417 East 68th Street, New York, NY 10065, USA;

[b]School of Medicine, University of Alabama at Birmingham, Birmingham, AL 35233, USA;

[c]Department of Radiology, University of Alabama at Birmingham, Birmingham, AL 35233, USA;

[d]Department of Chemistry, University of Alabama at Birmingham, Birmingham, AL 35205, USA;

[e]Molecular Pharmacology Program, Memorial Sloan Kettering Cancer Center, New York, NY 10065, USA;

[f]Weill Cornell Medical College, New York, NY 10065, USA

Keywords

PET imaging; Oncology; Cardiology; Neurodegenerative disease; Personalized medicine; Novel PET tracers

PROMINENT PET TRACERS IN ONCOLOGY

This article first discusses many of the most prominent PET imaging agents in late preclinical and early clinical development in oncology. These agents are intended to take advantage of the unique biological and physiologic characteristics of tumors to delineate malignant from normal tissues as a means of improving current methods of diagnosis. In addition, numerous PET imaging agents focus on probing the biological characteristics of cancers and other cell populations of interest in tumors to monitor and predict the efficacy of various therapeutic strategies.

Fibroblast Activation Protein Inhibitors

Cancer-associated fibroblasts and extracellular fibroblasts are among the most abundant cell types in solid cancers.[1] These cells, which dominate the tumor stoma, have been found to play a significant role in regulating the antitumor immune response and thus have been a noteworthy target of interest for both diagnostic and therapeutic applications.[1,2] Cancer-associated fibroblasts overexpress the fibroblast activation protein (FAP), which has led to the development of fibroblast-activating protein inhibitors (FAPIs), as a means of selectively

*Corresponding author. 417 East 68th Street, New York, NY 10065. lewisj2@mskcc.org.
[1]Present address: 1824 6th Avenue South, Birmingham, AL 35294.

DISCLOSURE

With regard to the information presented in this article the authors have no potential conflicts of interest to disclose.

targeting these cells to improve therapeutic outcomes.[3] Although therapeutic radionuclides attach via chelators to FAPI and have been evaluated in numerous types of cancer, the focus here is on PET imaging applications. An extensive amount of research has focused on the preclinical and clinical evaluation of variations of the [^{68}Ga]Ga-FAPI PET tracer, including [^{68}Ga]Ga-FAPI-2, [^{68}Ga]Ga-FAPI-4, [^{68}Ga]Ga-FAPI-46, and [^{68}Ga]Ga-FAPI-74 in various types of cancers.[4–14]

One such prominent study extensively assessed the use of [^{68}Ga]Ga-FAPI-04 as an imaging agent in 28 different types of cancers. Images generated from this study are shown in Fig. 1.[4] The standard uptake value (SUV) varied depending on the type of cancer, but the investigators reported tumor to background ratios greater than 3 for the moderate uptake groups and more than 6 for the high-intensity uptake groups.[4] In addition, studies have been performed directly comparing the imaging capabilities of [^{68}Ga]FAPI and [^{18}F]-fluorodeoxyglucose (FDG),[9,11,12] and some physicians argue that this tracer could replace [^{18}F]FDG, especially in cancers where surrounding tissues show high rates of metabolism resulting in high background signal.[15] More recent work has explored the capabilities of an ^{18}F-labeled FAPI imaging agent as a means of extending the radioactive half-life of the tracer to improve its availability to more remote locations.[14] The results of these studies have shown the potential of these tracers in numerous types of cancer for both diagnostic and staging applications. There are currently 20 active clinical trials exploring the use of FAPI PET imaging agents in various cancers and diseases. There is significant optimism that these tracers could play a prominent role in addressing pitfalls in current standard of care techniques and improve patient outcomes.

Imaging Increased Rates of Cellular Proliferation

The ^{18}F-labeled nucleoside analogue 3′-fluoro-3′deoxythymidine (FLT) is a PET imaging agent that has seen significant interest for its ability to quantify cellular proliferation. The capabilities of this tracer were initially reported in 1998, and have since sparked a large number of preclinical and clinical evaluations for its potential in overcoming the challenges associated with [^{18}F]FDG.[16] [^{18}F]FLT has the potential to better delineate malignant tissues in areas with high metabolic rates, such as muscle, lymphocytes, brain tissue, as well as in head and neck cancers.[17–19] In a clinical evaluation performed by Buck and colleagues,[20] the uptake of [^{18}F]FLT better correlated with staging than [^{18}F]FDG in soft tissue tumors, with mean SUVs of 0.7, 1.3, 4.1, and 6.1 in benign lesions, low-grade sarcoma, grade 2 tumors, and grade 3 tumors respectively.

In addition, the ability to monitor cell proliferation has made [^{18}F]FLT PET a promising tool to noninvasively monitor therapeutic response and predict outcomes in patients with a variety of cancers.[21] Numerous studies have been performed to evaluate the potential of [^{18}F]FLT to predict patient response to several treatment strategies. A recent study explored the use of [^{18}F]FLT PET imaging to determine response to neoadjuvant chemotherapy targeting the c-met pathway in soft tissue sarcomas.[19] Researchers observed, in a small subset of 15 patients, that 12 had observable changes in [^{18}F]FLT accumulation, 8 patients showed response, and 4 progressed. The results of this pilot study support the potential of this tracer to monitor response, and further evaluation of this tracer is currently being

explored.[19] [^{18}F]FLT has been evaluated in numerous types of cancer.[21] In some studies in head and neck cancer and non–small cell lung cancer, [^{18}F]FLT performs worse or about the same as [^{18}F]FDG in monitoring therapeutic response.[22,23] In other studies in patients with ovarian cancer and lymphoma, [^{18}F]FLT has better performance in determining therapeutic outcomes.[24,25] Although results can vary depending on the type of cancer and treatment strategy, [^{18}F]FLT is a prominent imaging agent that has significant potential in improving detection and monitoring therapeutic outcomes.

Prostate-Specific Membrane Antigen

The development of PET imaging agents targeting the prostate-specific membrane antigen (PSMA) has been an extensive area of research over the past decade, generating close to 1000 research articles in the past 2 years alone. PSMA PET imaging has been implemented in the clinic as an improved method of staging and restaging patients as well as to monitor for recurrence and metastatic dissemination after therapy.[26–28] More recent work has been designed to evaluate [^{68}Ga]PSMA PET imaging for initial diagnosis that could potentially improve detection of early-stage recurrence in patients with only moderately increased levels of prostate-specific antigen.[29] In addition, there is significant interest in using PSMA PET imaging to guide therapeutic strategies, such as radiotherapy and radioimmunotherapy, as well as predict patient outcomes.[30–32]

One of the most widely used PSMA targeted tracers is [^{68}Ga]PSMA-11, which is the focus of numerous preclinical and clinical studies and has recently been approved by the US Food and Drug Administration (FDA) in patients with suspected metastatic and recurrent prostate cancer. A more novel tracer, [^{18}F]PSMA-1007, is also being evaluated in the clinic and has the advantage of a longer physical half-life compared with [^{68}Ga]PSMA-11.[33] Another PSMA imaging agent in late phase development is [^{18}F]F-2-(3-{1-carboxy-5-[(6-[18F]fluoro-pyridine-3-carbonyl)-amino]-pentyl}-ureido)-pentanedioic acid (DCFPyL). In a study of 262 patients with biochemically recurrent prostate cancer, 91.4% of lesions with an SUV_{peak} greater than 3.5 and 95.5% of lesions with an SUV_{peak} greater than 4.0 were considered malignant on [^{18}F]F-DCFPyL PET.[34]

Although prostate cancer has been the main area of focus in most of the studies performed to date, more recent work has begun to elucidate the significance of PSMA expression in other types of cancers. PSMA expression in the neovasculature of many different cancers has been shown to be increased, and thus recent research has aimed to take advantage of this increased expression in cancers such as breast cancer, non–small cell lung cancer, colorectal cancer, renal cell carcinoma, pancreatic cancer, and highly vascularized gliomas, such as glioblastoma multiforme.[28,35,36] One such example includes a recent study evaluating the use of [^{68}Ga]PSMA-11 to detect and stage primary and metastatic breast cancer lesions.[37] The researchers reported promising detection rates in lesions identified by [^{18}F] FDG.[37] These results along with numerous preclinical and clinical evaluations support the prominent role PSMA targeted PET tracers may have on the diagnosis and therapeutic outcomes in patients with prostate cancer and other cancers with PSMA expression in their neovasculature.

Deltalike Protein 3

The deltalike protein 3 (DLL3) is an inhibitory ligand of the Notch pathway and is upregulated in 85% of small cell lung cancers and other neuroendocrine cancers, whereas nonneuroendocrine cancers and normal tissues do not express DLL3.[38] Castration-resistant neuroendocrine prostate cancers also show increased expression of DLL3 and thus this ligand has received attention in recent years for its potential as a target in immunotherapies such as rovalpituzumab teserine (SC16LD6.5),[39] and radioimmunotherapies including ^{225}Ac and ^{177}Lu labeled anti-DLL3 monoclonal antibodies.[40] Several multicenter clinical trials have been performed exploring the use of rovalpituzumab teserine as a therapy in small cell lung cancer.

The use of PET imaging to guide therapies is of significant interest in these indications because conventional methods of analyzing DLL3 expression are limited. These limitations include insufficient contemporaneous analysis of DLL3 expression, sampling bias resulting from intratumoral and intertumoral heterogeneity, and the inherently high false-negative rate for histopathologic assessment of DLL3 expression.[41] The implementation of PET imaging can overcome many of these limitations and thus has been of significant interest in this field. Sharma and colleagues[41] reported the preclinical evaluation of an [^{89}Zr]Zr-DFO-SC16 PET imaging agent in small cell lung cancer xenografts as a means of noninvasively quantifying DLL3 expression. In this work, statistically significant differences in tumor accumulation were observed between the high and low DLL3-expressing small cell lung cancer xenograft models. In addition, uptake of the [^{89}Zr]Zr-DFO-SC16 correlated with therapeutic response, highlighting the potential of these tracers to predict patient outcome.[41] With the promising results of this preclinical analysis, a clinical trial (NCT04199741) was initiated to evaluate the use of [^{89}Zr]Zr-DFO-SC16.56 to noninvasively monitor DLL3 expression in patients, and is currently ongoing.

Poly(ADP-ribose) Polymerase 1

Poly(ADP-ribose) polymerase 1 (PARP1) is part of a family of proteins tasked with repairing single-strand DNA breaks as part of the base excision repair pathway.[42] With increased rates of metabolism and proliferation, cancer cells are more prone to developing single-strand breaks and thus show increased expression and activity of PARP1.[43,44] The increased reliance on DNA repair pathways is a prominent characteristic of many types of cancer, and thus a significant amount of research has been aimed at targeting these pathways to prevent DNA repair, ultimately leading to cell death.[42,45–47] There are currently 4 FDA-approved inhibitors of PARP1: olaparib, niraparib, rucaparib, and talazoparib.[46]

A significant volume of research is focused on the development of imaging agents that are based on these PARP inhibitor (PARPi) scaffolds for their potential applications in cancer diagnosis, patient stratification, and monitoring therapy.[48] As a diagnostic, these imaging agents are particularly focused on improving current standard-of-care modalities such as [^{18}F]FDG, which has limitations in certain areas of the body because of high background signal in normal tissues. Several PARP-selective tracers have been developed and evaluated in preclinical and/or clinical studies, including [^{18}F]FluorThanatrace and [^{18}F]PARPi.[49–53] The [^{18}F]PARPi tracer was developed based on the FDA-approved olaparib scaffold, and

the [^{18}F]PARPi tracer was evaluated extensively in preclinical settings as a diagnostic and a means of monitoring the accumulation and retention of PARPi in the tumor.[54,55] This tracer has since been used in clinical trials (NCT04173104 and NCT03631017) for multiple types of cancer and has shown promising results, as shown in Fig. 2. Continued development of these tracers will likely lead to multiple novel radiotracers that can provide improved contrast in PET images, stratify patients, and identify tumors that are likely to respond to therapies targeting the PARP enzyme.

Immune Checkpoint Inhibitors

Immune checkpoint inhibitors such as programmed cell death protein 1 (PD-1)/programmed death-ligand 1 (PD-L1) and cytotoxic T lymphocyte–associated protein 4 (CTLA-4) have received significant attention for their impressive results in some patients.[56,57] However, one of the major limitations of these therapies is the lack of a marker that can be used to stratify patients who are likely to respond to immune checkpoint blockade.[58,59] There are several possible explanations as to why traditional immunohistochemistry quantification of expression for the ligands that play a role in immune activity does not correlate with patient outcomes. Many in the field believe that heterogeneous expression and the dynamic nature of the ligand expression are the leading factors preventing clinicians from determining whether a patient is likely to respond.[60,61] PET imaging has the potential of overcoming these 2 limitations and thus has led to a significant effort to develop an effective PET tracer that can noninvasively monitor expression and correlate well with patient outcomes.[62]

One strategy is to prepare ^{89}Zr-labeled monoclonal antibodies that selectively bind with the particular immune checkpoint ligand. There are several monoclonal antibodies to date that have been approved by the FDA for use in immune checkpoint therapies.[63] One such monoclonal antibody is pembrolizumab, one of the earliest FDA-approved and widely implemented immune checkpoint inhibitors.[63] There are several researchers who have prepared ^{89}Zr-labeled versions of the pembrolizumab antibody to evaluate its potential in quantifying PD-1 expression using varying approaches.[64–66] Several clinical trials (NCT02760225, NCT04605614, and NCT03065764) have also been initiated to evaluate PET tracers based on the pembrolizumab antibody in the clinic. Additional clinical trials are also underway for PET tracers based on other FDA-approved antibodies, including ipilimumab, atezolizumab, and avelumab.

Another prominent approach that has seen success in preclinical settings attempts to monitor T-cell activation as a consequence of immune checkpoint therapies using PET/computed tomography (CT) by administering the 18-fluoro-9-(β-D-arabinofuranosyl) guanine ([^{18}F]F-AraG) imaging agent. [^{18}F]F-AraG has been established as selective for activated T lymphocytes,[67] and accumulation of [^{18}F]F-AraG paralleled the course of adaptive immune response in a preclinical colorectal cancer model.[68] Multiple clinical trials are currently investigating the ability of this tracer to monitor T-cell activation in response to immune checkpoint blockade in several types of cancer.

Imaging Extracellular Acidic and Hypoxic Conditions

There are several distinct characteristics of cancer that allow researchers and clinicians to develop novel therapeutic and diagnostic agents that specifically target tumors. One such characteristic is the reduced pH and hypoxic conditions within the extracellular environment of most tumors as a result of the poorly formed vasculature as well as aberrant and increased rates of metabolism and cell proliferation.[69,70] This characteristic has led to a significant research effort to devise unique and clever ways to take advantage of this phenomenon. These efforts have brought to fruition numerous pH-sensitive cleavable linkers that can improve the selectivity and efficacy of drug molecules, peptides that can alter their structure as a result of pH and insert themselves into the membrane of cells, and radiolabeled molecules that are metabolized by cells that have altered metabolic pathways as a result of environmental stimuli.[70–76]

The evaluation of the family of pH (low) insertion peptides has produced promising results and has shown the capabilities of targeting the acidic microenvironment within tumors. These peptides alter their structures in a low-pH environment, forming a transmembrane alpha helix that inserts itself into the cell membrane.[72,73,77] These peptides have been labeled with several different isotopes for PET imaging, including ^{18}F and ^{64}Cu.[73,77] The research performed to date evaluating these peptides has focused on their potential as diagnostic agents as well as discerning which patients or tumors are likely to respond to pH low insertion peptide (pHLIP) variants designed for delivery of therapeutic payloads.[78] At present, a clinical trial has been initiated for an ^{18}F-labeled version of the pHLIP peptide to evaluate its efficacy for imaging the low-pH environments in patients with breast cancer (NCT04054986).

Another strategy for imaging tumor microenvironment focuses on the hypoxic conditions in the extracellular matrix and the variations in cell metabolism that result.[74,79] The tracer [^{18}F]fluoro-misonidazole ([^{18}F]FMISO) is reduced by hypoxic cells and accumulates in regions of the body where these conditions exist. Imaging hypoxia has several clinically relevant applications. These agents can act as a companion diagnostic in regions of the body where imaging metabolism using [^{18}F]FDG is insufficient in diagnosing cancer and/or the presence of hypoxia could alter the therapeutic plan.[80] Imaging hypoxia can act as a prognostic indicator and guide therapeutic strategy, and also has a significant impact on radiotherapy where hypoxic cells are much more radiation resistant than normoxic cells, thus requiring increased radiation dose to obtain sufficient therapeutic efficacy.[74] Although [^{18}F]FMISO seems to be the most prominent tracer currently being explored, many other tracers are also in development, including [^{18}F]fluoroazomycin arabinoside ([^{18}F]FAZA),[80–82] with numerous ongoing clinical trials such as NCT03418818, NCT04395469, and NCT02701699, and [^{64}Cu]Cu-diacetyl-bis(N4-methylthiosemicarbazone) ([^{64}Cu]Cu-ATSM)[83–85] also with ongoing clinical trials NCT03951337.

Radiolabeled Analogues of Bioactive Molecules

As researchers continue to elucidate the complex mechanisms involved in cancer biology and metabolism, many novel radiotracers have been developed based on bioactive molecules

such as amino acids, hormones, and antibodies that target or interact with processes more specifically associated with cancer. Many of the tracers mentioned previously would be considered among this class of tracers. Although a complete list of novel and promising PET tracers is beyond the scope of this article, briefly, the following tracers are examples of this diverse and powerful field and will likely make their way into clinical settings in the very near future if they have not already.

The PET tracers 3,4-dihydroxy-6[^{18}F]fluoro-L-phenylalanine ([^{18}F]FDOPA), L-[^{11}C]methionine ([^{11}C]MET), and O-(2-[^{18}F]fluoroethyl)-L-tyrosine ([^{18}F]F-FET) are amino acid analogues of particular interest for their potential in improving diagnosis of primary brain tumors, including glioblastoma.[86–90] These tracers improve on current standard of care because they are capable of passing through an intact blood-brain barrier and have much improved tumor/normal brain uptake ratio compared with [^{18}F]FDG. Each of these tracers is currently under investigation in ongoing clinical trials. Another example of radiolabeled amino acids is the (4*S*)-4-(3[^{18}F]fluoropropyl)-L-glutamic acid ([^{18}F]F-FSPG) PET tracer. This tracer is of particular interest for its ability to determine drug resistance because the tumor uptake can indicate the upregulation of antioxidant pathways. This tracer has been shown to provide an early indicator for tumor response in preclinical studies, preceding other standard methods such as tumor size regression or reduced glucose metabolism.[91] These results have led to several clinical trials that are evaluating the ability of these tracers to act as a diagnostic and monitor therapeutic response in patients.

A tracer that uses a radiolabeled hormone analogue is the 16α-[^{18}F]fluoroestradiol ([^{18}F]F-FES), which is capable of providing a method of noninvasively assessing estrogen expression within a tumor and was approved by the FDA in June of 2020. This tracer has been studied as a diagnostic for recurrent and metastatic breast cancer in patients with a history of estrogen-positive primary cancer.[92,93] Ongoing clinical trials, such as NCT02398773, are evaluating the ability of [^{18}F]FES to improve current diagnostic techniques for assessing recurrent and metastatic breast cancer as well as predict patient response to endocrine therapies. Additional hormone analogues currently under study include 21-[^{18}F]fluoro-furanyl-norprogesterone ([^{18}F]FFNP) as a means of evaluating progesterone expression in breast cancers (NCT03212170), as well as the 16β-[^{18}F]fluoro-5α-dihydrotestosterone ([^{18}F]F-FDHT) to diagnose recurrent and metastatic prostate cancer and evaluate androgen receptor expression to guide therapeutic strategies.[93–95] These tracers have provided promising results with high selectivity and sensitivity, noninvasive quantitation of receptor expression to inform therapeutic strategies, and the capability of monitoring changes in hormone receptor expression as a result of endocrine therapies.

Antibodies and the various fragments that can be engineered from portions of the antibody is an expansive and invaluable area of research that has generated an extensive and ever-growing library of highly specific therapeutic and diagnostic agents that have seen tremendous success in preclinical and clinical studies.[96] The investigators of the Antibodies to Watch series presented an excellent breakdown of the current field of antibody-based therapeutics for treatment in multiple diseases from academic and industrial laboratories that are at varying stages of clinical development.[96] As antibodies are evaluated and confirmed to

be effective therapeutics, novel PET imaging agents can readily be prepared by labeling these antibodies with chelators capable of incorporating radioactive isotopes. Thus, as the number of viable and effective therapeutic antibodies continues to grow, so does the library of imaging agents with the potential of improving diagnostic capabilities, stratifying patients who are more likely to respond to therapy, and more quickly and accurately monitoring patient response. Some examples of approved antibodies that have been adapted as PET imaging agents include [^{89}Zr]Zr-durvalumab for imaging PD-L1 expression in head and neck cancers as well as lymphoma (NCT03610061, NCT03829007), [^{89}Zr]Zr-ramucirumab for imaging VEGFR-2 expression in prostate cancer,[97] and [^{64}Cu]Cu-Bn-NOTA-hu14.18K322A, a humanized version of the chimeric antibody dinutuximab, used to image disialoganglioside GD2 expression in neuroblastoma and osteosarcoma.[98] In addition, some of the previously discussed imaging agents were developed from approved antibodies such as [^{89}Zr]Zr-atezolizumab (NCT04564482, NCT03850028, NCT04222426), [^{89}Zr]Zr-avelumab (NCT03514719), and [^{89}Zr]Zr-ipilimumab (NCT04029181, NCT03313323).

RADIOPHARMACEUTICALS FOR PET IMAGING IN NEUROLOGY

Highlighted here are the radiopharmaceuticals, for nononcology neurologic PET imaging, that are either FDA approved or in late-stage clinical trials. Nononcology neurologic PET imaging focuses on a range of neurologic disorders,[99,100] with an emphasis placed on neurodegenerative diseases such as Parkinson disease (PD) and Alzheimer disease (AD). Such neurodegenerative disorders are notable for the accumulation of protein inclusions in the brain and their impact on neurotransmission.

To illustrate this point, patients with PD experience a degeneration of the nigrostriatal pathway that results in the loss of dopaminergic neurons. This neuronal loss has been shown to correlate with the aggregation of protein α-synuclein in the neuronal perikarya, forming the characteristic Lewy body.[101] In addition, the primary pathology features of AD is the aggregate burden of 2 proteins: β-amyloid, the principal component of neurotic plaques, and tau protein, a component of neurofibrillary tangles.[102] Impairment of the cholinergic system is also thought to play a significant role in the cognitive decline experienced by patients with AD.[103]

These unique disease indications, in combination with the chronic inflammation they produce, are used as potential targets in the development and use of radiopharmaceuticals for the PET imaging of neurologic disorders.

Protein-Targeted Imaging

One of the primary pathology features in neurodegenerative diseases such as PD and AD is protein aggregation. Thus, protein-targeted imaging is an especially notable modality in AD, which has a significant aggregate burden of amyloid-beta (Aβ) plaques and tau protein. Note that preclinical targeting of the PD aggregate protein α-synuclein has met with limited success to date, with recent efforts showing promise.[104]

The clinical relevance of imaging agents targeting Aβ plaques and tau protein in AD are discussed next.

β-Amyloid imaging agents—The accumulation of β-amyloid into Aβ plaques is one of the hallmarks of AD. The first widely used PET imaging agent for detecting these plaques, [^{11}C]PiB (2-[4-([^{11}C]methylamino)phenyl]-1,3-benzothiazol-6-ol; Pittsburgh compound B), continues to have widespread use in research ever since its first use in human studies in the early 2000s.[105] Although this tracer is not approved for clinical use by the FDA, it is notable for its high specificity for Aβ plaques and ability to differentiate AD from other types of neurodegeneration that do not involve Aβ deposition, such as frontotemporal lobar degeneration (FTLD).[106] For this reason, [^{11}C]PiB has been used as a comparative standard in the development of new β-amyloid imaging agents. There is also increasing evidence for the presence of comorbidities in neurodegenerative disorders, such as the presence of Aβ plaques in some patients with PD.[107,108] [^{11}C]PiB is being used in clinical trials to measure the amyloid burden in PD (NCT03555292), to evaluate the potential presence of comorbid AD. The results of this trial could provide unique clinical insight into the disease burden of Aβ plaques in PD and other types of neurodegeneration.

Beyond [^{11}C]C-PiB, 3 ^{18}F-labeled amyloid imaging agents have been approved for use by the FDA, within the last decade, for the detection of Aβ plaques in patients undergoing evaluation for cognitive impairment with AD as a potential cause. These 3 tracers are [^{18}F]florbetapir (4-[(*E*)-2-[6-[2-[2-(2-[^{18}F]fluoranylethoxy)ethoxy]ethoxy]pyridin-3-yl]ethenyl]-*N*-methylaniline; Amyvid), [^{18}F]florbetaben (4-[(*E*)-2-[4-[2-[2-(2-[^{18}F]fluoranylethoxy)ethoxy]ethoxy]phenyl]ethenyl]-*N*-methylaniline; NeuraCeq), and [^{18}F]flutemetamol (2-[3-[^{18}F]fluoranyl-4-(methylamino)phenyl]-1,3-benzothiazol-6-ol; Vizamyl), and have proven efficacy in several clinical trials.[109–111] The tracers can be used to estimate the Aβ plaque density in patients with suspected AD but are not indicated to diagnose AD or other neurodegenerative disorders based on imaging alone. These 3 tracers continue to undergo clinical development and are commonly used as a standard with which to compare novel tracers. For example, florbetaben is being examined, similarly to [^{11}C]C-PiB, as a means to quantify the comorbid Aβ plaque burden experienced by patients with other neurodegenerative diseases, such as PD.[112]

There are 2 next-generation radiopharmaceuticals for imaging β-amyloid that have potential for clinical impact in the coming years: [^{18}F]FIBT (2-(*p*-methylaminophenyl)-7-(2-[^{18}F]fluoroethoxy)imidazo-[2,1-b]benzothiazole) and [^{18}F]NAV4694 (2-[2-[^{18}F]fluoro-6-(methylamino)-3-pyridinyl]-1-benzofuran-5-ol). In a human study involving 6 patients with AD, [^{18}F]FIBT showed imaging quality comparable with [^{11}C]PiB.[113] [^{18}F]FIBT was also shown to have a higher binding affinity and specificity for Aβ plaques. This study followed the first human study for [^{18}F]FIBT in 2015, which involved 2 patients: 1 patient with AD and 1 control. In this preliminary study, [^{18}F]FIBT was able to successfully differentiate the patient with AD from the control and showed a strong pattern of tracer uptake consistent with AD.[114] Because of the small number of subjects in these studies, larger clinical trials are required to further understand the utility of these agents.

The second radiopharmaceutical, [^{18}F]NAV4694 (also known as [^{18}F]AZD4694), has been shown to have imaging characteristics nearly identical to those of [^{11}C]PiB[115] and has recently undergone phase 2 and phase 3 trials (NCT01886820, NCT01680588). Despite its

demonstrated efficacy, a recently conducted human trial showed low uptake of the tracer in the preclinical phase of AD, suggesting a limit for its clinical use.[116] However, this tracer remains promising for future clinical use because of its favorable imaging characteristics.

Tau imaging agents—Tau protein is most associated with cognitive decline in neurodegenerative diseases such as AD. Note that tau protein accumulation is not a specific biomarker for AD; the protein is also present during acute brain conditions such as stroke.[117] In addition, different forms of tau accumulate in different neurodegenerative diseases, and PET tracers targeting tau typically bind preferentially to certain forms of tau.[118] However, research has shown that measuring the buildup of tau, which can occur before the formation of Aβ plaques, may be important in detecting AD in early stages.[119] Studies such as these suggest the important complementary role nonspecific protein imaging can play in disease-targeted imaging.

There are 3 radiopharmaceuticals that have been widely studied in the targeting of tau protein: [^{18}F]THK5351 ((2*S*)-1-[^{18}F]fluoranyl-3-[2-[6-(methylamino)pyridin-3-yl]quinolin-6-yl]oxypropan-2-ol), [^{18}F]AV1451 (7-(6-fluoropyridine-3-yl)-5*H*-pyrido[4,3-b]indole), [^{11}C]PBB3 (2-((1*E*,3*E*)-4-(6-((^{11}C-methylamino)pyridine-3-yl)buta-1,3-dienyl)benzo[d]thiazol-6-ol). In general, these 3 tracers were found to have excellent selectivity for tau protein compared with Aβ plaques with some off-target binding.[120] For example, [^{18}F]THK5351 binds to monoamine oxidase B and [^{11}C]PBB3 has been shown to bind to α-synuclein.[121] A study with [^{18}F]AV1451 involving 8 patients with AD and 8 healthy controls showed some age-related uptake of the compound among the healthy controls, indicating some off-target uptake.[122]

Beyond these 3 compounds, a new generation of tau tracers were designed to reduce off-target binding. Among these new radiopharmaceuticals, [^{18}F]MK-6240 (6-[^{18}F]fluoranyl-3-pyrrolo[2,3-c]pyridin-1-ylisoquinolin-5-amine) and [^{18}F]RO-6958948 (2-(6-[^{18}F]fluoro-pyridin-3-yl)-9H-1,6,9-triaza-fluorene) have shown promising results. The safety and efficacy of [^{18}F]MK-6240 has been shown preclinically[123] and is currently the subject of several active clinical trials (NCT04104659, NCT03706261). Large clinical trials have shown that [^{18}F]MK-6240 is able to identify individuals with AD with high fidelity and accuracy.[121] The tracer has also been an important tool in developing a better understanding of the role the tau protein plays in AD progression.

A human trial comparing [^{11}C]PiB and [^{18}F]MK-6240 showed patients with increased Aβ burden experience cognitive decline largely accounted for by the level of tau protein.[124] This trial highlights a potentially important role for future tau imaging to monitor disease progression. In addition, the short half-life of [^{11}C]PiB could allow the imaging of Aβ plaques and tau protein in the same patient on the same day (Fig. 3).

The tracer [^{18}F]RO-6958948 has undergone preclinical testing in mice, which showed its highly specific binding to tau and rapid kinetics.[125] The tracer has also recently completed several phase 1 trials testing for safety and efficiency in humans (NCT02792179, NCT02187627). Future clinical trials showing its clinical relevance in targeting tau protein are expected in the future.

Neurotransmission-Targeted Imaging

Dopaminergic system imaging—Patients with PD are known to experience a neurodegeneration affecting the nigrostriatal system, one of the 4 dopaminergic pathways in the brain. A well-established tracer for dopamine metabolism is [^{18}F]FDOPA.[126] This tracer is a substrate for aromatic acid decarboxylase (AADC), an enzyme necessary for the conversion of aromatic amino acids into neurotransmitters such as dopamine. This tracer was approved by the FDA in 2019 for the evaluation of adult patients with suspected parkinsonian syndromes, including PD, through the visualization dopaminergic nerve terminals. Human trials have shown that this tracer is both highly sensitive and highly specific.[127]

The design of the next generation of radiopharmaceuticals in this area is primarily focused on targeting 2 additional proteins: dopamine transporter (DAT) and vesicular monoamine transporter 2 (VMAT2). There are 2 novel tracers of interest related to these protein targets: [^{18}F]FP-CIT (methyl(1*R*,2*S*,3*S*,5*S*)-8-(3-fluoropropyl)-3-(4-[^{18}F]fluorophenyl)-8-azabicyclo[3.2.1]octane2-carboxylate) and [^{18}F]FE-PE2I ((*E*)-*N*-(3-iodoprop-2-enyl)-2β-carbo[^{18}F]fluoroethoxy-3β-(4′-methyl-phenyl)nortropane). In the case of FP-CIT, its ^{123}I-labeled form, ioflupane, is used clinically for single-photon emission computed tomography (SPECT) imaging in patients with suspected PD. An analysis of 6 PET clinical studies showed that [^{18}F]FP-CIT is a potential biomarker for early PD diagnosis.[128] In addition, a study with 9 patients with early PD was conducted using [^{18}F]FE-PE2I, which was successful in differentiating healthy controls and patients with early PD.[129] This same compound also showed good repeatability and reliability and is a possible marker to monitor the progress of DAT decline.[130] There has also been interest in imaging vesicular acetylcholine transporter, which has been associated with PD, using the PET ligand (2*R*,3*R*)-5-[^{18}F]fluoroethoxybenzovesamicol.[131]

Inflammation-Targeted Imaging and Synaptic Density

There is considerable evidence that both chronic inflammation[132] and reduced synaptic density[133] are associated with neurodegenerative disorders. As a result, there is interest in identifying markers for these two conditions associated with neurodegeneration. Of particular interest for inflammation is the translocator protein (TSPO) that is upregulated with high density in many neurologic disorders.[134] Markers of interest for synaptic density include high-density neural synapse proteins, one of which is synaptic vesicle protein 2A (SV2A).[135] The loss or decrease in density of these synaptic proteins indicates disease progression.

Translocator protein imaging—TSPO is a transmembrane protein upregulated during periods of neuroinflammation, following the activation of microglial cells.[134] One of the first radiopharmaceuticals targeting this protein was [^{11}C]PK-11195 (*N*-*sec*-butyl-1-(2-chlorophenyl)-*N*-[^{11}C]methyl-3-isoquinolinecarboxamide), which was widely used in research for several decades. However, clinical use of this compound was limited by nonspecific binding, low brain uptake, and the short half-life of ^{11}C.[136]

A second generation of TSPO-targeting radiopharmaceuticals was developed to address these limitations. Compounds in this second generation include [^{11}C]DAA1106 (*N*-(5-fluoro-2-phenoxyphenyl)-*N*-[(5-methoxy-2-[^{11}C]methoxyphenyl) methyl]acetamide), [^{11}C]PBR28 (*N*-[(2-[^{11}C]methoxyphenyl)methyl]-*N*-(6-phenoxypyridin-3-yl)acetamide), [^{18}F]FEPPA (*N*-[[2-(2-[^{18}F]fluoranylethoxy)phenyl]methyl]-*N*-(4-phenoxypyridin-3-yl)acetamide), [^{18}F]PBR06 (*N*-[(2,5-dimethoxyphenyl)methyl]-2-[^{18}F]fluoranyl-*N*-(2-phenoxyphenyl)acetamide), [^{18}F]PBR11 (2-(6-chloro-2-(4-(3-[^{18}F]fluoropropoxy)phenyl)imidazo[1,2-a]pyridin-3-yl)-*N*,*N*-diethylacetamide), and [^{18}F]DPA714 ([*N*,*N*-diethyl-2-(2-(4-(2[^{18}F]fluoroethoxy)phenyl)5,7dimethylpyrazolo[1,5a]pyrimidin-3-yl)acetamide]). Many of these new compounds showed higher brain uptake and greater specificity for the TSPO target compared with [^{11}C]PK-11195.[137] However, additional studies also revealed that genetic variation in the TSPO gene among participants resulted in TSPO expression with varied the binding affinity for the tracer, leading to the classification of so-called high-affinity, low-affinity, and mixed-affinity binding groups.[138] Patients with low-affinity TSPO binding present a significant clinical contraindication for TSPO-targeted imaging and have been excluded from some clinical trials. Despite this limitation, the largest improvement in TSPO-targeted imaging with second-generation radiopharmaceuticals was the development of ^{18}F-labeled compounds, which benefit from a longer half-life compared with their ^{11}C-labeled counterparts to allow more widespread use.

TSPO-targeted imaging studies of neurodegenerative disorders with second-generation DPA-714 modeled acute inflammation in rats and showed that [^{18}F]DPA-714 is a selective and reliable biomarker[139] with a more favorable signal/noise ratio than [^{11}C]PK-11195.[140] However, one of the first human trials, involving 10 patients with AD and 6 healthy controls, showed no significant difference in [^{18}F]DPA-714 uptake between the two groups.[141] Note that no information on the binding status of the participants of this trial was available for this study. A subsequent human trial, involving 64 patients with AD and 32 controls, specifically studied high-affinity and mixed-affinity binders. The results of the trial showed greater TSPO uptake among high-affinity and mixed-affinity binders compared with healthy controls and also showed that participants with a greater uptake of TSPO had a slower disease progression over a period of 2 years, indicating a possible protective effect provided by TSPO.[142] The results of these 2 clinical trials introduce new questions regarding the use of [^{18}F]DPA-714 in identifying neurodegeneration and the potential importance of binding status on TSPO-targeted imaging. Further exploration of this compound continues, including current clinical trials to determine whether patients who experience higher neuroinflammation have more symptoms from neuroinflammatory diseases (NCT03759522). Overall, the development of second-generation TSPO imaging agents has shown promise regarding binding specificity and brain uptake, but continued developments may improve image quality and diagnostic utility.[143]

Synaptic vesicle protein 2A—SV2A is a membrane protein localized to the synapse in neural cells.[135] Many neurodegenerative diseases are known to reduce the density of these synapses, thereby reducing the amount of SV2A.[144] As a result, SV2A has been investigated as a clinical marker for neurodegeneration.

Among the first-generation SV2A tracers, 3 have been identified with potential clinical relevance: [^{18}F]UCB-H, [^{11}C]UCB-A, and [^{11}C]UCB-J (4*R*)-1-(3-([^{11}C]methylpyridin-4-yl)methyl)-4-(3,4,5-trifluorophenyl)pyrrolidin-2-one. A preclinical analysis of these 3 compounds found [^{11}C]UCB-J to have superior imaging characteristics, including rapid brain uptake, and fast, reversible binding with high specificity to SV2A.[144] Compared with [^{11}C]UCB-J, [^{11}C]UCB-A was found to have a slower kinetics, whereas [^{18}F]UCB-H had less specific binding.

To date, there have been several clinical trials that have shown the efficacy of these 3 compounds as a diagnostic measure in neurodegenerative disorders (NCT03577262, NCT04243304). The safety and efficacy of [^{18}F]UCB-H as a means of studying synaptic density was first shown in a small human study involving 4 healthy subjects.[145] Similar efficacy was shown in a clinical trial of [^{11}C] UCB-J involving 10 patients with AD and 11 healthy controls, which found a significant reduction of SV2A in areas of the brain associated with the progression of AD disease.[146] A larger clinical trial of [^{18}F]UCB-H involving 24 patients with AD and 19 healthy controls also showed a significantly reduced uptake of the tracer in areas of the brain related to cognitive decline in patients with AD.[147]

Out of the 3 first-generation SV2A tracers, [^{11}C] UCB-J, is considered the best in its class because of its rapid uptake, fast kinetics, and specific binding. However, the short half-life of ^{11}C presents a limitation for widespread use, similar to the first-generation TSPO-targeting compound [^{11}C]PK-11195. Independent attempts to synthesize a longer-lived ^{18}F derivative were met with success by 2 research groups, who synthesized a compound that was jointly named [^{18}F]SynVesT-1 (4*R*)-1-(3-([^{18}F]methylpyridin-4-yl)methyl)-4-(3,4,5-trifluorophenyl)pyrrolidin-2-one.[148] In a preliminary study comparing the efficacy of [^{18}F]FSDM-8 and [^{11}C]UCB-J, the former was found to have imaging properties comparable with the first-generation compound with the added benefit of a longer half-life.[149] Current clinical trials with this second generation of SV2A tracers are ongoing or recently completed (NCT03587649).

RADIOPHARMACEUTICALS FOR CARDIOVASCULAR PET IMAGING

Most cardiac PET imaging has focused on blood flow (^{82}Rb and [^{13}N]NH_3) and metabolism ([^{18}F] FDG). Research into newer agents for both of these areas continues and is complemented by additional compounds in imaging of atherosclerosis and angiogenesis.

PET Agents for Myocardial Perfusion Imaging

Although the approval of ^{82}Rb and [^{13}N]NH_3 has enabled widespread cardiac PET imaging, the very short half-lives of ^{82}Rb and ^{13}N make these studies accessible only at sites with access to an ^{82}Sr/^{82}Rb generator or an on-site cyclotron. Thus, there has been significant research into longer-lived imaging agents for this purpose.

[^{18}F]Flurpiridaz (2-*tert*-butyl-4-chloro-5-[4-(2-[^{18}F]fluoroethoxymethyl)-benzyloxy]-2H-pyridazin-3–1) is under investigation for myocardial perfusion imaging in late-stage clinical trials.[150] A phase III clinical trial recently reported that, although the imaging study was not as specific as other available agents, the sensitivity was significantly higher than SPECT

agents, as shown in Fig. 4. Studies comparing imaging characteristics of [^{18}F]flurpiridaz with those of [^{13}N]NH_3 showed no significant differences between parameters derived from images with either agent.[151] Other agents labeled with ^{18}F and ^{68}Ga are also under investigation in preclinical studies.[152,153]

PET Agents for Imaging of Cardiac Metabolism

[^{18}F]FDG is widely available and has been used for cardiac metabolism and sarcoidosis. However, complementary agents have provided additional insight into cardiac function.

[^{11}C]Acetate has long been used for imaging of metabolism in a variety of disease states. In the research setting, this imaging strategy has been used to study cardiac metabolism in several investigations. For example, in a study of asymptomatic men with chromic alcohol consumption, investigators showed that [^{11}C]acetate PET/CT could be used to detect metabolic changes in the myocardium.[154] Newer imaging analysis techniques combined with dynamic imaging have also shown the feasibility of oxygen consumption, myocardial external efficiency, and blood flow in a single scan.[155,156]

Imaging of fatty acid metabolism has also been an ongoing area of study in cardiac research. In particular, [^{11}C]palmitate has been used for many years in basic metabolism studies.[157] In a multiple tracer study involving [^{15}O]water and [1-^{11}C] glucose, palmitate, and leucine, investigators were able to image myocardial metabolic changes associated with Barth syndrome.[158] Newer fatty acid agents such as [^{18}F]fluoro-4-thiapalmitate (FTP) are also being studied in ongoing clinical trials in cardiac metabolism. In a paired study with lean controls and diabetic glycemically controlled volunteers, investigators found fatty acid oxidation was higher in the diabetic group and could be altered in both groups by the administration of insulin.[159]

PET Agents for Imaging of Cardiovascular Disease

As mentioned earlier, there are several agents that have shown utility in assessment of amyloid burden in patients with cognitive impairment. Atherosclerosis has also been shown to contain amyloid proteins. Thus, imaging using previously developed agents for β-amyloid has been investigated in atherosclerosis and cardiac amyloidosis. Other biomarkers, including CCR2, are also currently being studied.

Amyloid imaging—Preliminary human imaging studies using [^{18}F]flutemetamol showed visible uptake in carotid arteries, with male gender associated with enhanced uptake.[160] In a recent study in patients with suspected cardiac amyloidosis, imaging with [^{18}F]florbetaben at delayed timepoints allowed the differentiation of immunoglobulin light chain–derived amyloidosis from transthyretin-related amyloidosis.[161] Similar results were also reported using [^{11}C]PiB in multiple studies.[162,163] However, in several recent [^{18}F]flutemetamol studies in patients with cardiac amyloidosis, results were mixed, with 1 group reporting that PET/CT could be used to differentiate between patients with transthyretin amyloidosis and another reporting that the diagnostic yield from images acquired was low.[164,165] Additional clinical trials in this area are ongoing (NCT01683825, NCT04105634, NCT02641145, NCT04392960).

Other targets in atherosclerosis—Macrophages and other inflammatory cells are known to be associated with atherosclerotic processes.[166] Existing agents targeting TSPO and somatostatin receptors have been investigated for imaging of inflammatory processes with some success in preclinical models and several clinical trials.[166] For example, in a study involving 42 patients with atherosclerosis [^{68}Ga]DOTATATE out-performed [^{18}F]FDG for the evaluation of high-risk versus low-risk coronary lesions (NCT02021188).[167] Newer agents such as [^{64}Cu] DOTA-ECL1i, which targets CCR2, are currently in clinical trials (NCT04537403) in patients with carotid and femoral artery disease.

Prominent and novel tracers, along with their current status, are listed in Table 1.

Abbreviation Chemical Name

FAPI	Fibroblast activation protein inhibitor
FLT	3′-Fluoro-3′ deoxythymidine
FDG	Fluorodeoxyglucose
PSMA	Prostate-specific membrane antigen
[^{18}F]DCFPyL	2-(3-{1-carboxy-5-[(6-[^{18}F]fluoro-pyridine-3-carbonyl)-amino]-pentyl}-ureido)-pentanedioic acid
DFO	Deferoxamine
DLL3	Deltalike protein 3
PARP1	Poly(ADP-ribose) polymerase 1
[^{18}F]F-AraG	[^{18}F]fluoro-9-(β-D-arabinofuranosyl) guanine
pHLIP	pH low insertion peptide
[^{18}F]FMISO	[^{18}F]fluoro-misonidazole
[^{18}F]FAZA	[^{18}F]fluoroazomycin arabinoside
[^{64}Cu]Cu-ATSM	[^{64}Cu]Cu-diacetyl-bis(N^4-methylthiosemicarbazone)
[^{11}C]MET	L-[^{11}C]methionine
[^{18}F]FET	*O*-(2-[^{18}F]fluoroethyl)-L-tyrosine
[^{18}F]FSPG	(4*S*)-4-(3[^{18}F]fluoropropyl)-L-glutamic acid
[^{18}F]FES	16α-[^{18}F]fluoroestradiol
[^{18}F]FFNP	21-[^{18}F]F-fluoro-furanyl-norprogesterone
[^{18}F]FDHT	16β-[^{18}F]F-fluoro-5α-dihydrotestosterone
[^{11}C]PiB	2-[4-([^{11}C]methylamino)phenyl]-1,3-benzothiazol-6-ol

[^{18}F]Florbetapir	4-[(*E*)-2-[6-[2-[2-(2-[^{18}F]fluoranylethoxy)ethoxy]ethoxy]pyridin-3-yl]ethenyl]-*N*-methylaniline
[^{18}F]Florbetaben	4-[(*E*)-2-[4-[2-[2-(2-[^{18}F]fluoranylethoxy)ethoxy]ethoxy]phenyl]ethenyl]-*N*-methylaniline
[^{18}F]Flutemetamol	2-[3-[^{18}F]fluoranyl-4-(methylamino)phenyl]-1,3-benzothiazol-6-ol
[^{18}F]FIBT	2-(*p*-Methylaminophenyl)-7-(2-[^{18}F]fluoroethoxy)imidazo-[2,1-b]benzothiazole
[^{18}F]NAV4694	2-[2-^{18}F-fluoro-6-(methylamino)-3-pyridinyl]-1-benzofuran-5-ol
[^{18}F]THK5351	(2*S*)-1-[^{18}F]fluoranyl-3-[2-[6-(methylamino)pyridin-3-yl]quinolin-6-yl]oxypropan-2-ol 7-(6-fluoropyridine-3-yl)-5H-pyrido[4,3-b]indole
[^{11}C]PBB3	2-((1*E*,3*E*)-4-(6-(^{11}C-methylamino)pyridine-3-yl)buta-1,3-dienyl)benzo[d]thiazol-6-ol
[^{18}F]MK-6240	6-[^{18}F]fluoranyl-3-pyrrolo[2,3-c]pyridin-1-ylisoquinolin-5-amine
[^{18}F]Ro-6958948	2-(6-[^{18}F]fluoro-pyridin-3-yl)-9H-1,6,9-triaza-fluorene
[^{18}F]FDOPA	(2*S*)-2-amino-3-(2-[^{18}F]fluoro-4,5-dihydroxyphenyl)propanoic acid
[^{18}F]FP-CIT	Methyl(1*R*,2*S*,3*S*,5*S*)-8-(3-fluoropropyl)-3-(4-[^{18}F]fluorophenyl)-8-azabicyclo [3.2.1]octane2-carboxylate
[^{18}F]FE-PE2I	(*E*)-N-(3-iodoprop-2-enyl)-2β-carbo[^{18}F]fluoroethoxy-3β-(4′-methyl-phenyl)nortropane)
[^{18}F]FEOBV	(2*R*,3*R*)-5-[^{18}F]fluoroethoxybenzovesamicol
[^{11}C]CPK-11195	*N*-*sec*-Butyl-1-(2-chlorophenyl)-*N*-[^{11}C]methyl-3-isoquinolinecarboxamide
[^{11}C]DAA1106	*N*-(5-Fluoro-2-phenoxyphenyl)-N-[(5-methoxy-2-[^{11}C]methoxyphenyl)methyl] acetamide

[^{11}C]PBR28	*N*-[(2-[^{11}C]methoxyphenyl)methyl]-*N*-(6-phenoxypyridin-3-yl)acetamide
[^{18}F]FEPPA	*N*-[[2-(2-[^{18}F]fluoranylethoxy)phenyl]methyl]-*N*-(4-phenoxypyridin-3-yl)acetamide
[^{18}F]PBR06	*N*-[(2,5-Dimethoxyphenyl)methyl]-2-[^{18}F]fluoranyl-*N*-(2-phenoxyphenyl)acetamide
[^{18}F]PBR11	2-(6-Chloro-2-(4-(3-[^{18}F]fluoropropoxy)phenyl)imidazo[1,2-a]pyridin-3-yl)-*N*, *N*-diethylacetamide
[^{18}F]DPA714	[N,N-diethyl-2-(2-(4-(2[18F]fluoroethoxy)phenyl)5,7dimethylpyrazolo[1,5a] pyrimidin-3-yl)acetamide]
[^{11}C]UCB-J	(4R)-1-((3-([11C]methylpyridin-4-yl)methyl)-4-(3,4,5-trifluorophenyl)pyrrolidin-2-one
[^{18}F]SynVesT-1	(4R)-1-((3-([18F]methylpyridin-4-yl)methyl)-4-(3,4,5-trifluorophenyl)pyrrolidin-2-one

REFERENCES

1. Liu T, Han C, Wang S, et al. Cancer-associated fibroblasts: an emerging target of anti-cancer immunotherapy. J Hematol Oncol 2019;12(1):86. [PubMed: 31462327]
2. Ziani L, Chouaib S, Thiery J. Alteration of the antitumor immune response by cancer-associated fibroblasts. Front Immunol 2018;9:414. [PubMed: 29545811]
3. Lindner T, Loktev A, Giesel F, et al. Targeting of activated fibroblasts for imaging and therapy. EJNMMI Radiopharmacy Chem 2019;4(1):16.
4. Kratochwil C, Flechsig P, Lindner T, et al. 68)Ga-FAPI PET/CT: Tracer Uptake in 28 Different Kinds of Cancer. J Nucl Med 2019;60(6):801–5. [PubMed: 30954939]
5. Giesel FL, Kratochwil C, Lindner T, et al. 68)Ga-FAPI PET/CT: Biodistribution and Preliminary Dosimetry Estimate of 2 DOTA-Containing FAP-Targeting Agents in Patients with Various Cancers. J Nucl Med 2019;60(3):386–92. [PubMed: 30072500]
6. Koerber SA, Staudinger F, Kratochwil C, et al. The Role of (68)Ga-FAPI PET/CT for Patients with Malignancies of the Lower Gastrointestinal Tract: First Clinical Experience. J Nucl Med 2020;61(9): 1331–6. [PubMed: 32060216]
7. Ballal S, Yadav MP, Kramer V, et al. A theranostic approach of [(68)Ga]Ga-DOTA.SA.FAPi PET/CT-guided [(177)Lu]Lu-DOTA.SA.FAPi radionuclide therapy in an end-stage breast cancer patient: new frontier in targeted radionuclide therapy. Eur J Nucl Med Mol Imaging 2020. 10.1007/s00259-020-04990-w.
8. Luo Y, Pan Q, Yang H, et al. Fibroblast activation protein targeted PET/CT with (68)Ga-FAPI for imaging IgG4-related disease: comparison to (18)F-FDG PET/CT. J Nucl Med 2020. 10.2967/jnumed.120.244723.
9. Pang Y, Zhao L, Chen H. 68Ga-FAPI Outperforms 18F-FDG PET/CT in identifying bone metastasis and peritoneal carcinomatosis in a patient with metastatic breast cancer. Clin Nucl Med 2020; 45(11):913–5. [PubMed: 32910045]
10. Shi X, Xing H, Yang X, et al. Comparison of PET imaging of activated fibroblasts and 18F-FDG for diagnosis of primary hepatic tumours: a prospective pilot study. Eur J Nucl Med Mol Imaging 2020. 10.1007/s00259-020-05070-9.

11. Pang Y, Hao B, Shang Q, et al. Comparison of 68Ga-FAPI and 18F-FDG PET/CT in a Patient With Cholangiocellular Carcinoma: A Case Report. Clin Nucl Med 2020;45(7):566–7. [PubMed: 32371618]
12. Chen H, Pang Y, Wu J, et al. Comparison of [(68) Ga]Ga-DOTA-FAPI-04 and [(18)F] FDG PET/CT for the diagnosis of primary and metastatic lesions in patients with various types of cancer. Eur J Nucl Med Mol Imaging 2020;47(8):1820–32. [PubMed: 32222810]
13. Meyer C, Dahlbom M, Lindner T, et al. Radiation Dosimetry and Biodistribution of (68)Ga-FAPI-46 PET Imaging in Cancer Patients. J Nucl Med 2020;61(8):1171–7. [PubMed: 31836685]
14. Giesel F, Adeberg S, Syed M, et al. FAPI-74 PET/CT Using Either (18)F-AlF or Cold-kit (68)Ga-labeling: Biodistribution, Radiation Dosimetry and Tumor Delineation in Lung Cancer Patients. J Nucl Med 2020. 10.2967/jnumed.120.245084.
15. Calais J, Mona CE. Will FAPI PET/CT Replace FDG PET/CT in the Next Decade?—Point: An Important Diagnostic, Phenotypic and Biomarker Role. AJR Am J Roentgenol 2020. 10.2214/AJR.20.24302.
16. Shields AF, Grierson JR, Dohmen BM, et al. Imaging proliferation in vivo with [F-18]FLT and positron emission tomography. Research Support, U.S. Gov't, P.H.S. Nat Med 1998;4(11):1334–6. [PubMed: 9809561]
17. Bashir A, Vestergaard MB, Marner L, et al. PET imaging of meningioma with 18F-FLT: a predictor of tumour progression. Brain 2020. 10.1093/brain/awaa267.
18. Rybka J, Małkowski B, Olejniczak M, et al. Comparing radioactive tracers 18F-FDG and 18F-FLT in the staging of diffuse large B-cell lymphoma by PET/CT examination: A single-center prospective study. Adv Clin Exp Med 2019;28(8):1095–9. [PubMed: 31237123]
19. Kairemo K, Santos EB, Macapinlac HA, et al. Molecular Imaging with 3'-deoxy-3'[(18)F]-Fluorothymidine ((18)F-FLT) PET/CT for Early Response to Targeted Therapies in Sarcomas: A Pilot Study. Diagnostics (Basel) 2020;10(3). 10.3390/diagnostics10030125.
20. Buck AK, Herrmann K, Büschenfelde CMz, et al. Imaging Bone and Soft Tissue Tumors with the Proliferation Marker [18F]Fluorodeoxythymidine. Clin Cancer Res 2008;14(10):2970. [PubMed: 18445694]
21. Peck M, Pollack HA, Friesen A, et al. Applications of PET imaging with the proliferation marker [18F]-FLT. Q J Nucl Med 2015;59(1):95–104.
22. Hoshikawa H, Kishino T, Mori T, et al. The value of 18F-FLT PET for detecting second primary cancers and distant metastases in head and neck cancer patients. Clin Nucl Med 2013;38(8): e318–23. [PubMed: 23455521]
23. Bhoil A, Singh B, Singh N, et al. Can 3'-deoxy-3'-(18)F-fluorothymidine or 2'-deoxy-2'-(18)F-fluorod-glucose PET/CT better assess response after 3-weeks treatment by epidermal growth factor receptor kinase inhibitor, in non-small lung cancer patients? Preliminary results. Hell J Nucl Med 2014; 17(2):90–6. [PubMed: 24997081]
24. Tsuyoshi H, Morishita F, Orisaka M, et al. 18F-fluorothymidine PET is a potential predictive imaging biomarker of the response to gemcitabine-based chemotherapeutic treatment for recurrent ovarian cancer: preliminary results in three patients. Clin Nucl Med 2013;38(7):560–3. [PubMed: 23640220]
25. Lee H, Kim SK, Kim YI, et al. Early determination of prognosis by interim 3'-deoxy-3'-18F-fluorothymidine PET in patients with non-Hodgkin lymphoma. J Nucl Med 2014;55(2):216–22. [PubMed: 24365650]
26. Afshar-Oromieh A, Haberkorn U, Hadaschik B, et al. PET/MRI with a 68Ga-PSMA ligand for the detection of prostate cancer. Eur J Nucl Med Mol Imaging 2013;40(10):1629–30. [PubMed: 23817686]
27. Barakat A, Yacoub B, Homsi ME, et al. Role of Early PET/CT Imaging with 68Ga-PSMA in Staging and Restaging of Prostate Cancer. Sci Rep 2020; 10(1):2705. [PubMed: 32066750]
28. Sasikumar A Specificity of (68)Ga-PSMA PET/CT for Prostate Cancer - Myths and Reality. Indian J Nucl Med 2017;32(1):11–2. [PubMed: 28242976]
29. Plouznikoff N, Artigas C, Sideris S, et al. Early Detection of Metastatic Prostate Cancer Relapse on 68Ga-PSMA-11 PET/CT in a Patient Still Exhibiting Biochemical Response. Clin Nucl Med 2020; 45(1):81–2. [PubMed: 31693605]

30. Emmett L, van Leeuwen PJ, Nandurkar R, et al. Treatment Outcomes from (68)Ga-PSMA PET/CT-Informed Salvage Radiation Treatment in Men with Rising PSA after radical prostatectomy: prognostic value of a negative PSMA PET. J Nucl Med 2017;58(12):1972–6. [PubMed: 28747524]
31. Roberts MJ, Morton A, Donato P, et al. 68)Ga-PSMA PET/CT tumour intensity pre-operatively predicts adverse pathological outcomes and progression-free survival in localised prostate cancer. Eur J Nucl Med Mol Imaging 2020. 10.1007/s00259-020-04944-2.
32. Michalski K, Mix M, Meyer PT, et al. Determination of whole-body tumour burden on [68Ga]PSMA-11 PET/CT for response assessment of [177Lu] PSMA-617 radioligand therapy: a retrospective analysis of serum PSA level and imaging derived parameters before and after two cycles of therapy. Nuklearmedizin 2019;58(6):443–50. Bestimmung der mittels [68Ga]PSMA-11 PET/CT bestimmten Ganzkörper-Tumorlast zur Abschätzung des Therapieansprechens: Eine retrospektive Analyse des Serum-PSA-Wertes und bildgebender Parameter vor und nach 2 Zyklen [177Lu]PSMA-617-Radioligandentherapie. [PubMed: 31724145]
33. Witkowska-Patena E, Giżewska A, Dziuk M, et al. Diagnostic performance of 18F-PSMA-1007 PET/CT in biochemically relapsed patients with prostate cancer with PSA levels ≤ 2.0 ng/ml. Prostate Cancer Prostatic Dis 2020;23(2):343–8. [PubMed: 31780781]
34. Meijer D, Jansen BHE, Wondergem M, et al. Clinical verification of 18F-DCFPyL PET-detected lesions in patients with biochemically recurrent prostate cancer. PLoS One 2020;15(10):e0239414. [PubMed: 33021980]
35. Tolkach Y, Gevensleben H, Bundschuh R, et al. Prostate-specific membrane antigen in breast cancer: a comprehensive evaluation of expression and a case report of radionuclide therapy. Breast Cancer Res Treat 2018;169(3):447–55. [PubMed: 29455299]
36. Salas Fragomeni RA, Amir T, Sheikhbahaei S, et al. Imaging of nonprostate cancers using PSMA-Targeted Radiotracers: Rationale, Current State of the Field, and a Call to Arms. J Nucl Med 2018; 59(6):871–7. [PubMed: 29545375]
37. Medina-Ornelas S, García-Perez F, Estrada-Lobato E, et al. (68)Ga-PSMA PET/CT in the evaluation of locally advanced and metastatic breast cancer, a single center experience. Am J Nucl Med Mol Imaging 2020;10(3):135–42. [PubMed: 32704404]
38. Chen B, Li H, Liu C, et al. Potential prognostic value of delta-like protein 3 in small cell lung cancer: a meta-analysis. World J Surg Oncol 2020;18(1):226. [PubMed: 32847588]
39. Rudin CM, Pietanza MC, Bauer TM, et al. Rovalpituzumab tesirine, a DLL3-targeted antibody-drug conjugate, in recurrent small-cell lung cancer: a first-in-human, first-in-class, open-label, phase 1 study. Lancet Oncol 2017;18(1):42–51. [PubMed: 27932068]
40. Lakes AL, An DD, Gauny SS, et al. Evaluating (225) Ac and (177)Lu Radioimmunoconjugates against Antibody-Drug Conjugates for Small-Cell Lung Cancer. Mol Pharm 2020;17(11):4270–9. [PubMed: 33044830]
41. Sharma SK, Pourat J, Abdel-Atti D, et al. Noninvasive Interrogation of DLL3 Expression in Metastatic Small Cell Lung Cancer. Cancer Res 2017;77(14):3931–41. [PubMed: 28487384]
42. Chan CY, Tan KV, Cornelissen B. PARP Inhibitors in Cancer Diagnosis and Therapy. Clin Cancer Res 2020. 10.1158/1078-0432.Ccr-20-2766.
43. Liu Y, Zhang Y, Zhao Y, et al. High PARP-1 expression is associated with tumor invasion and poor prognosis in gastric cancer. Oncol Lett 2016; 12(5):3825–35. [PubMed: 27895737]
44. Ossovskaya V, Koo IC, Kaldjian EP, et al. Upregulation of Poly (ADP-Ribose) Polymerase-1 (PARP1) in Triple-Negative Breast Cancer and Other Primary Human Tumor Types. Genes Cancer 2010;1(8):812–21. [PubMed: 21779467]
45. Slade D PARP and PARG inhibitors in cancer treatment. Genes Dev 2020;34(5–6):360–94. [PubMed: 32029455]
46. Sachdev E, Tabatabai R, Roy V, et al. PARP Inhibition in Cancer: An Update on Clinical Development. Target Oncol 2019;14(6):657–79. [PubMed: 31625002]
47. Ellisen LW. PARP inhibitors in cancer therapy: promise, progress, and puzzles. Cancer Cell 2011;19(2):165–7. [PubMed: 21316599]
48. Carney B, Kossatz S, Reiner T. Molecular Imaging of PARP. J Nucl Med 2017;58(7):1025–30. [PubMed: 28473593]

49. Michel LS, Dyroff S, Brooks FJ, et al. PET of Poly (ADP-Ribose) Polymerase Activity in Cancer: Preclinical Assessment and First In-Human Studies. Radiology 2017;282(2):453–63. [PubMed: 27841728]
50. Zhou D, Xu J, Mpoy C, et al. Preliminary evaluation of a novel (18)F-labeled PARP-1 ligand for PET imaging of PARP-1 expression in prostate cancer. Nucl Med Biol 2018;66:26–31. [PubMed: 30195072]
51. Demétrio de Souza França P, Roberts S, Kossatz S, et al. Fluorine-18 labeled poly (ADP-ribose) polymerase1 inhibitor as a potential alternative to 2-deoxy-2-[(18)F]fluoro-d-glucose positron emission tomography in oral cancer imaging. Nucl Med Biol 2020;84–85:80–7. [PubMed: 33189948]
52. Salinas B, Irwin CP, Kossatz S, et al. Radioiodinated PARP1 tracers for glioblastoma imaging. EJNMMI Res 2015;5(1):123. [PubMed: 26337803]
53. Sander Effron S, Makvandi M, Lin L, et al. PARP-1 Expression Quantified by [(18)F]FluorThanatrace: A Biomarker of Response to PARP Inhibition Adjuvant to Radiation Therapy. Cancer Biother Radiopharm 2017;32(1):9–15. [PubMed: 28118040]
54. Carney B, Kossatz S, Lok BH, et al. Target engagement imaging of PARP inhibitors in small-cell lung cancer. Nat Commun 2018;9(1):176. [PubMed: 29330466]
55. Laird J, Lok BH, Carney B, et al. Positron-Emission Tomographic Imaging of a Fluorine 18-Radiolabeled Poly(ADP-Ribose) Polymerase 1 Inhibitor Monitors the Therapeutic Efficacy of Talazoparib in SCLC Patient-Derived Xenografts. J Thorac Oncol 2019;14(10):1743–52. [PubMed: 31195178]
56. Kalbasi A, Ribas A. Tumour-intrinsic resistance to immune checkpoint blockade. Nat Rev Immunol 2020;20(1):25–39. [PubMed: 31570880]
57. Wieder T, Eigentler T, Brenner E, et al. Immune checkpoint blockade therapy. J Allergy Clin Immunol 2018;142(5):1403–14. [PubMed: 29596939]
58. Zappasodi R, Wolchok JD, Merghoub T. Strategies for Predicting Response to Checkpoint Inhibitors. Curr Hematol Malig Rep 2018;13(5):383–95. [PubMed: 30159703]
59. Lang D, Wahl G, Poier N, et al. Impact of PET/CT for Assessing Response to Immunotherapy-A Clinical Perspective. J Clin Med 2020;9(11). 10.3390/jcm9113483.
60. Nimmagadda S Quantifying PD-L1 expression to monitor immune checkpoint therapy: opportunities and challenges. Cancers (Basel) 2020;12(11).
61. Franzin R, Netti GS, Spadaccino F, et al. The use of immune checkpoint inhibitors in oncology and the occurrence of AKI: where do we stand? Review. Front Immunol 2020;11(2619). 10.3389/fimmu.2020.574271.
62. Miao Y, Lv G, Chen Y, et al. One-step radiosynthesis and initial evaluation of a small molecule PET tracer for PD-L1 imaging. Bioorg Med Chem Lett 2020;30(24):127572. [PubMed: 32979488]
63. Marhelava K, Pilch Z, Bajor M, et al. Targeting Negative and Positive Immune Checkpoints with Monoclonal Antibodies in Therapy of Cancer. Cancers 2019;11(11):1756.
64. Li W, Wang Y, Rubins D, et al. PET/CT Imaging of (89)Zr-N-sucDf-Pembrolizumab in Healthy Cynomolgus Monkeys. Mol Imaging Biol 2020. 10.1007/s11307-020-01558-w.
65. England CG, Ehlerding EB, Hernandez R, et al. Preclinical Pharmacokinetics and Biodistribution Studies of 89Zr-Labeled Pembrolizumab. J Nucl Med 2017;58(1):162–8. [PubMed: 27493273]
66. van der Veen EL, Giesen D, Pot-de Jong L, et al. 89)Zr-pembrolizumab biodistribution is influenced by PD-1-mediated uptake in lymphoid organs. J Immunother Cancer 2020;8(2). 10.1136/jitc-2020-000938.
67. Namavari M, Chang YF, Kusler B, et al. Synthesis of 2'-deoxy-2'-[18F]fluoro-9-β-D-arabinofuranosyl-guanine: a novel agent for imaging T-cell activation with PET. Mol Imaging Biol 2011;13(5):812–8. [PubMed: 20838911]
68. Levi J, Lam T, Goth SR, et al. Imaging of Activated T Cells as an Early Predictor of Immune Response to Anti-PD-1 Therapy. Cancer Res 2019;79(13): 3455–65. [PubMed: 31064845]
69. Kato Y, Ozawa S, Miyamoto C, et al. Acidic extracellular microenvironment and cancer. Cancer Cell Int 2013;13(1):89. [PubMed: 24004445]
70. Boedtkjer E, Pedersen SF. The Acidic Tumor Microenvironment as a Driver of Cancer. Annu Rev Physiol 2020;82:103–26. [PubMed: 31730395]

71. Reshetnyak YK, Moshnikova A, Andreev OA, et al. Targeting Acidic Diseased Tissues by pH-Triggered Membrane-Associated Peptide Folding. Review. Front Bioeng Biotechnol 2020;8:335. [PubMed: 32411684]
72. Weerakkody D, Moshnikova A, Thakur MS, et al. Family of pH (low) insertion peptides for tumor targeting. Proc Natl Acad Sci U S A 2013;110(15): 5834–9. [PubMed: 23530249]
73. Demoin DW, Wyatt LC, Edwards KJ, et al. PET Imaging of Extracellular pH in Tumors with (64)Cu- and (18)F-Labeled pHLIP Peptides: A Structure-Activity Optimization Study. Bioconjug Chem 2016;27(9):2014–23. [PubMed: 27396694]
74. Rajendran JG, Krohn KA. F-18 fluoromisonidazole for imaging tumor hypoxia: imaging the microenvironment for personalized cancer therapy. Semin Nucl Med 2015;45(2):151–62. [PubMed: 25704387]
75. Zhao G, Long L, Zhang L, et al. Smart pH-sensitive nanoassemblies with cleavable PEGylation for tumor targeted drug delivery. Sci Rep 2017;7(1): 3383. [PubMed: 28611459]
76. Wang J, Wen Y, Zheng L, et al. Characterization of chemical profiles of pH-sensitive cleavable D-gluconhydroximo-1, 5-lactam hydrolysates by LC–MS: A potential agent for promoting tumor-targeted drug delivery. J Pharm Biomed Anal 2020;185:113244. [PubMed: 32193041]
77. Shan L (64)Cu-1,4,7,10-Tetraazacyclododecane-1,4,7-Tris-acetic acid-10-maleimidoethylacetamide-ACEQNPIYWARYADWLFTTP LLLLDLALLVDADEGTG. Molecular imaging and contrast agent Database (MICAD). National Center for Biotechnology Information (US); 2004.
78. Wyatt LC, Lewis JS, Andreev OA, et al. Applications of pHLIP Technology for Cancer Imaging and Therapy. Trends Biotechnol 2017;35(7): 653–64. [PubMed: 28438340]
79. Lee ST, Scott AM. Hypoxia positron emission tomography imaging with 18F-fluoromisonidazole. Semin Nucl Med 2007;37(6):451–61. [PubMed: 17920352]
80. Theodoropoulos AS, Gkiozos I, Kontopyrgias G, et al. Modern radiopharmaceuticals for lung cancer imaging with positron emission tomography/computed tomography scan: A systematic review. SAGE Open Med 2020;8. 2050312120961594.
81. Melsens E, De Vlieghere E, Descamps B, et al. Hypoxia imaging with (18)F-FAZA PET/CT predicts radiotherapy response in esophageal adenocarcinoma xenografts. Radiat Oncol 2018;13(1):39. [PubMed: 29514673]
82. Mapelli P, Picchio M. 18F-FAZA PET imaging in tumor hypoxia: A focus on high-grade glioma. Int J Biol Markers 2020;35(1_suppl):42–6. [PubMed: 32079461]
83. Vavere AL, Lewis JS. Cu-ATSM: a radiopharmaceutical for the PET imaging of hypoxia. Dalton Trans 2007;(43):4893–902. [PubMed: 17992274]
84. Bourgeois M, Rajerison H, Guerard F, et al. Contribution of [64Cu]-ATSM PET in molecular imaging of tumour hypoxia compared to classical [18F]-MISO–a selected review. Nucl Med Rev Cent East Eur 2011;14(2):90–5. [PubMed: 22219149]
85. Kalinauskaite G, Senger C, Kluge A, et al. 68Ga-PSMA-PET/CT-based radiosurgery and stereotactic body radiotherapy for oligometastatic prostate cancer. PLoS One 2020;15(10):e0240892. [PubMed: 33085712]
86. Xiao J, Jin Y, Nie J, et al. Diagnostic and grading accuracy of (18)F-FDOPA PET and PET/CT in patients with gliomas: a systematic review and meta-analysis. BMC Cancer 2019;19(1):767. [PubMed: 31382920]
87. Cicone F, Carideo L, Scaringi C, et al. Long-term metabolic evolution of brain metastases with suspected radiation necrosis following stereotactic radiosurgery: longitudinal assessment by F-DOPA-PET. Neuro Oncol 2020. 10.1093/neuonc/noaa239.
88. Zaragori T, Ginet M, Marie P-Y, et al. Use of static and dynamic [(18)F]-F-DOPA PET parameters for detecting patients with glioma recurrence or progression. EJNMMI Res 2020;10(1):56. [PubMed: 32472232]
89. Cai L, Gao S, Li DC, et al. [Value of 18F-FDG and 11C-MET PET-CT in differentiation of brain ringlike-enhanced neoplastic and non-neoplastic lesions on MRI imaging]. Zhonghua Zhong Liu Za Zhi 2009;31(2):134–8. [PubMed: 19538892]
90. Muoio B, Giovanella L, Treglia G. Recent Developments of 18F-FET PET in Neuro-oncology. Curr Med Chem 2018;25(26):3061–73. [PubMed: 29173147]

91. Park SY, Mosci C, Kumar M, et al. Initial evaluation of (4S)-4-(3-[(18)F]fluoropropyl)-L-glutamate (FSPG) PET/CT imaging in patients with head and neck cancer, colorectal cancer, or non-Hodgkin lymphoma. EJNMMI Res 2020;10(1):100. [PubMed: 32857284]
92. Peterson LM, Kurland BF, Yan F, et al. 18)F-Fluoroestradiol ((18)F-FES)-PET imaging in a Phase II trial of vorinostat to restore endocrine sensitivity in ER+/HER2− metastatic breast cancer. J Nucl Med 2020. 10.2967/jnumed.120.244459.
93. Katzenellenbogen JA. PET Imaging Agents (FES, FFNP, and FDHT) for Estrogen, Androgen, and Progesterone Receptors to Improve Management of Breast and Prostate Cancers by Functional Imaging. Cancers 2020;12(8):2020.
94. Salem K, Kumar M, Yan Y, et al. Sensitivity and Isoform Specificity of (18)F-Fluorofuranylnorprogester-one for Measuring Progesterone Receptor Protein Response to Estradiol Challenge in Breast Cancer. J Nucl Med 2018. 10.2967/jnumed.118.211516.
95. McHugh DJ, Chudow J, DeNunzio M, et al. A Phase I Trial of IGF-1R Inhibitor Cixutumumab and mTOR inhibitor temsirolimus in metastatic castration-resistant prostate cancer. Clin Genitourin Cancer 2020;18(3):171–8.e2. [PubMed: 32057715]
96. Kaplon H, Muralidharan M, Schneider Z, et al. Antibodies to watch in 2020. mAbs 2020;12(1): 1703531. [PubMed: 31847708]
97. Li M, Jiang D, Barnhart TE, et al. Immuno-PET imaging of VEGFR-2 expression in prostate cancer with (89)Zr-labeled ramucirumab. Am J Cancer Res 2019;9(9):2037–46. [PubMed: 31598404]
98. Butch ER, Mead PE, Amador Diaz V, et al. Positron Emission Tomography Detects *In Vivo* Expression of Disialoganglioside GD2 in Mouse Models of Primary and Metastatic Osteosarcoma. Cancer Res 2019;79(12):3112–24. [PubMed: 31015228]
99. Holland N, Jones PS, Savulich G, et al. Synaptic Loss in Primary Tauopathies Revealed by [(11) C] UCB-J Positron Emission Tomography. Mov Disord 2020;35(10):1834–42. [PubMed: 32652635]
100. Cybulska K, Perk L, Booij J, et al. Huntington's Disease: A Review of the Known PET Imaging Biomarkers and Targeting Radiotracers. Molecules 2020;25(3). 10.3390/molecules25030482.
101. Kovacs GG, Milenkovic IJ, Preusser M, et al. Nigral burden of alpha-synuclein correlates with striatal dopamine deficit. Mov Disord 2008;23(11): 1608–12. [PubMed: 18649394]
102. Bondi MW, Edmonds EC, Salmon DP. Alzheimer's Disease: Past, Present, and Future. J Int Neuropsychol Soc 2017;23(9–10):818–31. [PubMed: 29198280]
103. Ferreira-Vieira TH, Guimaraes IM, Silva FR, et al. Alzheimer's disease: Targeting the Cholinergic System. Curr Neuropharmacol 2016;14(1):101–15. [PubMed: 26813123]
104. Maurer A, Leonov A, Ryazanov S, et al. (11) C Radiolabeling of anle253b: a Putative PET Tracer for Parkinson's Disease That Binds to α-Synuclein Fibrils in vitro and Crosses the Blood-Brain Barrier. ChemMedChem 2020;15(5):411–5. [PubMed: 31859430]
105. Klunk WE, Engler H, Nordberg A, et al. Imaging brain amyloid in Alzheimer's disease with Pittsburgh Compound-B. Ann Neurol 2004;55(3): 306–19. [PubMed: 14991808]
106. Rabinovici GD, Furst AJ, O'Neil JP, et al. 11C-PIB PET imaging in Alzheimer disease and frontotemporal lobar degeneration. Neurology 2007;68(15): 1205–12. [PubMed: 17420404]
107. Lashley T, Holton JL, Gray E, et al. Cortical alpha-synuclein load is associated with amyloid-beta plaque burden in a subset of Parkinson's disease patients. Acta Neuropathol 2008;115(4):417–25. [PubMed: 18185940]
108. Colom-Cadena M, Grau-Rivera O, Planellas L, et al. Regional Overlap of Pathologies in Lewy Body Disorders. J Neuropathol Exp Neurol 2017; 76(3):216–24. [PubMed: 28395086]
109. Clark CM, Pontecorvo MJ, Beach TG, et al. Cerebral PET with florbetapir compared with neuropathology at autopsy for detection of neuritic amyloid-β plaques: a prospective cohort study. Lancet Neurol 2012;11(8):669–78. [PubMed: 22749065]
110. Leinonen V, Rinne JO, Wong DF, et al. Diagnostic effectiveness of quantitative [^{18}F]flutemetamol PET imaging for detection of fibrillar amyloid β using cortical biopsy histopathology as the standard of truth in subjects with idiopathic normal pressure hydrocephalus. Acta Neuropathol Commun 2014; 2:46. [PubMed: 24755237]

111. Sabri O, Sabbagh MN, Seibyl J, et al. Florbetaben PET imaging to detect amyloid beta plaques in Alzheimer's disease: phase 3 study. Alzheimers Dement 2015;11(8):964–74. [PubMed: 25824567]
112. Yoo HS, Lee S, Chung SJ, et al. Dopaminergic Depletion, β-Amyloid Burden, and Cognition in Lewy Body Disease. Ann Neurol 2020;87(5):739–50. [PubMed: 32078179]
113. Grimmer T, Shi K, Diehl-Schmid J, et al. (18)F-FIBT may expand PET for β-amyloid imaging in neurodegenerative diseases. Mol Psychiatry 2018. 10.1038/s41380-018-0203-5.
114. Yousefi BH, Manook A, Grimmer T, et al. Characterization and first human investigation of FIBT, a novel fluorinated Aβ plaque neuroimaging PET radioligand. ACS Chem Neurosci 2015;6(3):428–37. [PubMed: 25482310]
115. Rowe CC, Pejoska S, Mulligan RS, et al. Head-to-head comparison of 11C-PiB and 18F-AZD4694 (NAV4694) for β-amyloid imaging in aging and dementia. J Nucl Med 2013;54(6):880–6. [PubMed: 23575995]
116. McSweeney M, Pichet Binette A, Meyer PF, et al. Intermediate flortaucipir uptake is associated with Aβ-PET and CSF tau in asymptomatic adults. Neurology 2020;94(11):e1190–200. [PubMed: 32015176]
117. Lee JC, Kim SJ, Hong S, et al. Diagnosis of Alzheimer's disease utilizing amyloid and tau as fluid biomarkers. Exp Mol Med 2019;51(5):1–10.
118. Robertson JS, Rowe CC, Villemagne VL. Tau imaging with PET: an overview of challenges, current progress, and future applications. Q J Nucl Med Mol Imaging 2017;61(4):405–13. [PubMed: 28750496]
119. Ritchie C, Smailagic N, Noel-Storr AH, et al. CSF tau and the CSF tau/ABeta ratio for the diagnosis of Alzheimer's disease dementia and other dementias in people with mild cognitive impairment (MCI). Cochrane Database Syst Rev 2017;3(3):Cd010803. [PubMed: 28328043]
120. Hall B, Mak E, Cervenka S, et al. In vivo tau PET imaging in dementia: Pathophysiology, radiotracer quantification, and a systematic review of clinical findings. Ageing Res Rev 2017;36:50–63. [PubMed: 28315409]
121. Pascoal TA, Therriault J, Benedet AL, et al. 18F-MK-6240 PET for early and late detection of neurofibrillary tangles. Brain 2020;143(9):2818–30. [PubMed: 32671408]
122. Barret O, Alagille D, Sanabria S, et al. Kinetic Modeling of the Tau PET Tracer (18)F-AV-1451 in Human Healthy Volunteers and Alzheimer Disease Subjects. J Nucl Med 2017;58(7):1124–31. [PubMed: 27908967]
123. Koole M, Lohith TG, Valentine JL, et al. Preclinical Safety Evaluation and Human Dosimetry of [(18)F] MK-6240, a Novel PET Tracer for Imaging Neurofibrillary Tangles. Mol Imaging Biol 2020;22(1):173–80. [PubMed: 31111397]
124. Betthauser TJ, Koscik RL, Jonaitis EM, et al. Amyloid and tau imaging biomarkers explain cognitive decline from late middle-age. Brain 2020;143(1):320–35. [PubMed: 31886494]
125. Gobbi LC, Knust H, Körner M, et al. Identification of Three Novel Radiotracers for Imaging Aggregated Tau in Alzheimer's Disease with Positron Emission Tomography. J Med Chem 2017;60(17):7350–70. [PubMed: 28654263]
126. Loane C, Politis M. Positron emission tomography neuroimaging in Parkinson's disease. Am J Transl Res 2011;3(4):323–41. [PubMed: 21904653]
127. Ibrahim N, Kusmirek J, Struck AF, et al. The sensitivity and specificity of F-DOPA PET in a movement disorder clinic. Am J Nucl Med Mol Imaging 2016; 6(1):102–9. [PubMed: 27069770]
128. Kong Y, Zhang C, Liu K, et al. Imaging of dopamine transporters in Parkinson disease: a meta-analysis of (18) F/(123) I-FP-CIT studies. Ann Clin Transl Neurol 2020. 10.1002/acn3.51122.
129. Delva A, Van Weehaeghe D, van Aalst J, et al. Quantification and discriminative power of (18)F-FE-PE2I PET in patients with Parkinson's disease. Eur J Nucl Med Mol Imaging 2020;47(8):1913–26. [PubMed: 31776633]
130. Kerstens VS, Fazio P, Sundgren M, et al. Reliability of dopamine transporter PET measurements with [(18)F]FE-PE2I in patients with Parkinson's disease. EJNMMI Res 2020;10(1):95. [PubMed: 32797307]
131. Bohnen NI, Kanel P, Zhou Z, et al. Cholinergic system changes of falls and freezing of gait in Parkinson's disease. Ann Neurol 2019;85(4):538–49. [PubMed: 30720884]

132. DeLegge MH. Smoke A. Neurodegeneration and inflammation. Nutr Clin Pract 2008;23(1):35–41. [PubMed: 18203962]
133. Jackson J, Jambrina E, Li J, et al. Targeting the Synapse in Alzheimer's Disease. Front Neurosci 2019;13:735. [PubMed: 31396031]
134. Schain M, Kreisl WC. Neuroinflammation in Neurodegenerative Disorders-a Review. Curr Neurol Neurosci Rep 2017;17(3):25. [PubMed: 28283959]
135. Madeo M, Kovács AD, Pearce DA. The human synaptic vesicle protein, SV2A, functions as a galactose transporter in Saccharomyces cerevisiae. J Biol Chem 2014;289(48):33066–71. [PubMed: 25326386]
136. Best L, Ghadery C, Pavese N, et al. New and Old TSPO PET Radioligands for Imaging Brain Microglial Activation in Neurodegenerative Disease. Curr Neurol Neurosci Rep 2019;19(5):24. [PubMed: 30941587]
137. Knezevic D, Mizrahi R. Molecular imaging of neuroinflammation in Alzheimer's disease and mild cognitive impairment. Prog Neuropsychopharmacol Biol Psychiatry 2018;80(Pt B):123–31. [PubMed: 28533150]
138. Guo Q, Owen DR, Rabiner EA, et al. Identifying improved TSPO PET imaging probes through biomathematics: the impact of multiple TSPO binding sites in vivo. Neuroimage 2012;60(2): 902–10. [PubMed: 22251896]
139. Rodríguez-Chinchilla T, Quiroga-Varela A, Molinet-Dronda F, et al. [(18)F]-DPA-714 PET as a specific in vivo marker of early microglial activation in a rat model of progressive dopaminergic degeneration. Eur J Nucl Med Mol Imaging 2020. 10.1007/s00259-020-04772-4.
140. Chauveau F, Van Camp N, Dollé F, et al. Comparative evaluation of the translocator protein radioligands 11C-DPA-713, 18F-DPA-714, and 11C-PK11195 in a rat model of acute neuroinflammation. J Nucl Med 2009;50(3):468–76. [PubMed: 19223401]
141. Golla SS, Boellaard R, Oikonen V, et al. Quantification of [18F]DPA-714 binding in the human brain: initial studies in healthy controls and Alzheimer's disease patients. J Cereb Blood Flow Metab 2015;35(5):766–72. [PubMed: 25649991]
142. Hamelin L, Lagarde J, Dorothée G, et al. Early and protective microglial activation in Alzheimer's disease: a prospective study using 18F-DPA-714 PET imaging. Brain 2016;139(Pt 4):1252–64. [PubMed: 26984188]
143. Dimitrova-Shumkovska J, Krstanoski L, Veenman L. Diagnostic and Therapeutic Potential of TSPO Studies Regarding Neurodegenerative Diseases, Psychiatric Disorders, Alcohol Use Disorders, Traumatic Brain Injury, and Stroke: An Update. Cells 2020;9(4). 10.3390/cells9040870.
144. Cai Z, Li S, Matuskey D, et al. PET imaging of synaptic density: A new tool for investigation of neuropsychiatric diseases. Neurosci Lett 2019;691:44–50. [PubMed: 30075287]
145. Bahri MA, Plenevaux A, Aerts J, et al. Measuring brain synaptic vesicle protein 2A with positron emission tomography and [(18)F]UCB-H. Alzheimers Dement (N Y) 2017;3(4):481–6. [PubMed: 29124105]
146. Chen MK, Mecca AP, Naganawa M, et al. Assessing Synaptic Density in Alzheimer Disease With Synaptic Vesicle Glycoprotein 2A Positron Emission Tomographic Imaging. JAMA Neurol 2018; 75(10):1215–24. [PubMed: 30014145]
147. Bastin C, Bahri MA, Meyer F, et al. In vivo imaging of synaptic loss in Alzheimer's disease with [18F] UCB-H positron emission tomography. Eur J Nucl Med Mol Imaging 2020;47(2):390–402. [PubMed: 31468182]
148. Nabulsi NB, Mercier J, Holden D, et al. Synthesis and Preclinical Evaluation of 11C-UCB-J as a PET Tracer for Imaging the Synaptic Vesicle Glycoprotein 2A in the Brain. J Nucl Med 2016;57(5):777–84. [PubMed: 26848175]
149. Li S, Cai Z, Wu X, et al. Synthesis and in Vivo Evaluation of a Novel PET Radiotracer for Imaging of Synaptic Vesicle Glycoprotein 2A (SV2A) in Nonhuman Primates. ACS Chem Neurosci 2019;10(3):1544–54. [PubMed: 30396272]
150. Packard RRS, Cooke CD, Van Train KF, et al. Development, diagnostic performance, and interob-server agreement of a (18)F-flurpiridaz PET automated perfusion quantitation system. J Nucl Cardiol 2020. 10.1007/s12350-020-02335-6.

151. Wang J, Mpharm SL, Liu TW, et al. Preliminary and Comparative Experiment Study Between (18)F-Flurpiridaz and (13)N-NH(3·)H(2)O Myocardial Perfusion Imaging With PET/CT in Miniature Pigs. Mol Imaging 2020;19. 1536012120947506.
152. Jammaz IA, Al-Otaibi B, Al-Hokbani N, et al. Synthesis of novel gallium-68 labeled rhodamine: A potential PET myocardial perfusion agent. Appl Radiat Isot 2019;144:29–33. [PubMed: 30508730]
153. Sivapackiam J, Laforest R, Sharma V. (68)Ga[Ga]-Galmydar: Biodistribution and radiation dosimetry studies in rodents. Nucl Med Biol 2018;59:29–35. [PubMed: 29454148]
154. Liu S, Lin X, Shi X, et al. Myocardial tissue and metabolism characterization in men with alcohol consumption by cardiovascular magnetic resonance and 11C-acetate PET/CT. J Cardiovasc Magn Reson 2020;22(1):23. [PubMed: 32299425]
155. Wu KY, Dinculescu V, Renaud JM, et al. Repeatable and reproducible measurements of myocardial oxidative metabolism, blood flow and external efficiency using (11)C-acetate PET. J Nucl Cardiol 2018;25(6):1912–25. [PubMed: 29453603]
156. Harms HJ, Hansson NHS, Kero T, et al. Automatic calculation of myocardial external efficiency using a single (11)C-acetate PET scan. J Nucl Cardiol 2018;25(6):1937–44. [PubMed: 29946824]
157. Christensen NL, Jakobsen S, Schacht AC, et al. Whole-Body Biodistribution, Dosimetry, and Metabolite Correction of [(11)C]Palmitate: A PET Tracer for Imaging of Fatty Acid Metabolism. Mol Imaging 2017;16.1536012117734485.
158. Cade WT, Laforest R, Bohnert KL, et al. Myocardial glucose and fatty acid metabolism is altered and associated with lower cardiac function in young adults with Barth syndrome. J Nucl Cardiol 2019. 10.1007/s12350-019-01933-3.
159. Mather KJ, Hutchins GD, Perry K, et al. Assessment of myocardial metabolic flexibility and work efficiency in human type 2 diabetes using 16-[18F]fluoro-4-thiapalmitate, a novel PET fatty acid tracer. Am J Physiol Endocrinol Metab 2016; 310(6):E452–60. [PubMed: 26732686]
160. Bucerius J, Barthel H, Tiepolt S, et al. Feasibility of in vivo (18)F-florbetaben PET/MR imaging of human carotid amyloid-b. Eur J Nucl Med Mol Imaging 2017;44(7):1119–28. [PubMed: 28321471]
161. Genovesi D, Vergaro G, Giorgetti A, et al. [18F]-Florbetaben PET/CT for Differential Diagnosis Among Cardiac Immunoglobulin Light Chain, Transthyretin Amyloidosis, and Mimicking Conditions. JACC Cardiovasc Imaging 2020. 10.1016/j.jcmg.2020.05.031.
162. Takasone K, Katoh N, Takahashi Y, et al. Non-invasive detection and differentiation of cardiac amyloidosis using (99m)Tc-pyrophosphate scintigraphy and (11)C-Pittsburgh compound B PET imaging. Amyloid 2020;1–9. 10.1080/13506129.2020.1798223. [PubMed: 31766892]
163. Rosengren S, Skibsted Clemmensen T, Tolbod L, et al. Diagnostic Accuracy of [(11)C]PIB positron emission tomography for detection of cardiac amyloidosis. JACC Cardiovasc Imaging 2020; 13(6):1337–47. [PubMed: 32417330]
164. Papathanasiou M, Kessler L, Carpinteiro A, et al. (18)F-flutemetamol positron emission tomography in cardiac amyloidosis. J Nucl Cardiol 2020. 10.1007/s12350-020-02363-2.
165. Möckelind S, Axelsson J, Pilebro B, et al. Quantification of cardiac amyloid with [(18)F]Flutemetamol in patients with V30M hereditary transthyretin amyloidosis. Amyloid 2020;27(3):191–9. [PubMed: 32400202]
166. Ćorović A, Wall C, Mason JC, et al. Novel Positron Emission Tomography Tracers for Imaging Vascular Inflammation. Curr Cardiol Rep 2020; 22(10):119. [PubMed: 32772188]
167. Tarkin JM, Joshi FR, Evans NR, et al. Detection of Atherosclerotic Inflammation by (68)Ga-DOTATATE PET Compared to [(18)F]FDG PET Imaging. J Am Coll Cardiol 2017;69(14):1774–91. [PubMed: 28385306]
168. Syed M, Flechsig P, Liermann J, et al. Fibroblast activation protein inhibitor (FAPI) PET for diagnostics and advanced targeted radiotherapy in head and neck cancers. Eur J Nucl Med Mol Imaging 2020;47(12):2836–45. [PubMed: 32447444]
169. Giesel FL, Heussel CP, Lindner T, et al. FAPI-PET/CT improves staging in a lung cancer patient with cerebral metastasis. Eur J Nucl Med Mol Imaging 2019;46(8):1754–5. [PubMed: 31119317]

170. Chen H, Zhao L, Ruan D, et al. 68Ga-FAPI PET/CT improves therapeutic strategy by detecting a second primary malignancy in a patient with rectal cancer. Clin Nucl Med 2020;45(6):468–70. [PubMed: 32149789]
171. Luo Y, Pan Q, Zhang W, et al. Intense FAPI uptake in inflammation may mask the tumor activity of pancreatic cancer in 68Ga-FAPI PET/CT. Clin Nucl Med 2020;45(4):310–1. [PubMed: 31977474]
172. Pang Y, Huang H, Fu L, et al. 68Ga-FAPI PET/CT detects gastric signet-ring cell carcinoma in a patient previously treated for prostate cancer. Clin Nucl Med 2020;45(8):632–5. [PubMed: 32453079]
173. Varasteh Z, Mohanta S, Robu S, et al. Molecular imaging of fibroblast activity after myocardial infarction using a (68)Ga-labeled fibroblast activation protein inhibitor, FAPI-04. J Nucl Med 2019; 60(12):1743–9. [PubMed: 31405922]
174. Novy Z, Stepankova J, Hola M, et al. Preclinical evaluation of radiolabeled peptides for PET imaging of glioblastoma multiforme. Molecules 2019; 24(13).
175. Kenny L The use of novel PET tracers to image breast cancer biologic processes such as proliferation, DNA damage and repair, and angiogenesis. J Nucl Med 2016;57(Suppl 1):89s–95s. [PubMed: 26834108]
176. O'Sullivan CC, Lindenberg M, Bryla C, et al. ANG1005 for breast cancer brain metastases: correlation between (18)F-FLT-PET after first cycle and MRI in response assessment. Breast Cancer Res Treat 2016;160(1):51–9. [PubMed: 27620882]
177. Kairemo K, Santos EB, Macapinlac HA, et al. Early response assessment to targeted therapy using 3'-deoxy-3'[(18)F]-fluorothymidine ((18)F-FLT) PET/CT in lung cancer. Diagnostics (Basel) 2020;10(1).
178. Campbell BA, Hofman MS, Prince HM. A novel application of [18F]Fluorothymidine-PET ([18F] FLT-PET) in clinical practice to quantify regional bone marrow function in a patient with treatment-induced cytopenias and to guide "marrow-sparing" radiotherapy. Clin Nucl Med 2019;44(11):e624–6. [PubMed: 31584492]
179. Kumar A, Ballal S, Yadav MP, et al. 177Lu-/68Ga-PSMA theranostics in recurrent glioblastoma multiforme: proof of concept. Clin Nucl Med 2020; 45(12):e512–3. [PubMed: 32558721]
180. Arslan E, Ergül N, Karagöz Y, et al. Recurrent brain metastasis of triple negative breast cancer with high uptake in 68Ga-PSMA-11 PET/CT. Clin Nucl Med 2020.
181. Korsen J, Kalidindi T, Khitrov S, et al. Delta-like ligand 3 (DLL3) is a novel target for molecular imaging of neuroendocrine prostate cancer. J Nucl Med 2020;61(supplement 1):133.
182. Puca L, Gavyert K, Sailer V, et al. Delta-like protein 3 expression and therapeutic targeting in neuroendocrine prostate cancer. Sci Transl Med 2019; 11(484).
183. Donabedian PL, Kossatz S, Engelbach JA, et al. Discriminating radiation injury from recurrent tumor with [(18)F]PARPi and amino acid PET in mouse models. EJNMMI Res 2018;8(1):59. [PubMed: 29974335]
184. Reilly SW, Puentes LN, Schmitz A, et al. Synthesis and evaluation of an AZD2461 [(18)F]PET probe in non-human primates reveals the PARP-1 inhibitor to be non-blood-brain barrier penetrant. Bioorg Chem 2019;83:242–9. [PubMed: 30390553]
185. Edmonds CE, Makvandi M, Lieberman BP, et al. [(18)F]FluorThanatrace uptake as a marker of PARP1 expression and activity in breast cancer. Am J Nucl Med Mol Imaging 2016;6(1):94–101. [PubMed: 27069769]
186. Miedema IH, Zwezerijnen GJ, Dongen GAv, et al. Abstract 1136: tumor uptake and biodistribution of ^{89}Zirconium-labeled ipilimumab in patients with metastatic melanoma during ipilimumab treatment. Cancer Res 2019;79(13 Supplement):1136.
187. Bensch F, van der Veen EL, Lub-de Hooge MN, et al. 89)Zr-atezolizumab imaging as a non-invasive approach to assess clinical response to PD-L1 blockade in cancer. Nat Med 2018;24(12): 1852–8. [PubMed: 30478423]
188. Li M, Ehlerding EB, Jiang D, et al. In vivo characterization of PD-L1 expression in breast cancer by immuno-PET with (89)Zr-labeled avelumab. Am J Transl Res 2020;12(5):1862–72. [PubMed: 32509182]

189. Jagoda EM, Vasalatiy O, Basuli F, et al. Immuno-PET imaging of the programmed cell death-1 ligand (PD-L1) using a zirconium-89 labeled therapeutic antibody, avelumab. Mol Imaging 2019;18. 1536012119829986.

190. Daumar P, Wanger-Baumann CA, Pillarsetty N, et al. Efficient (18)F-labeling of large 37-amino-acid pHLIP peptide analogues and their biological evaluation. Bioconjug Chem 2012;23(8):1557–66. [PubMed: 22784215]

191. Bittner MI, Wiedenmann N, Bucher S, et al. Analysis of relation between hypoxia PET imaging and tissue-based biomarkers during head and neck radiochemotherapy. Acta Oncol 2016;55(11):1299–304. [PubMed: 27593107]

192. Cheng J, Zhang J, He S, et al. Characterization of heterogeneity of hypoxia with 18FMISO PET/CT, BOLD fMRI and immunohistochemistry in human breast tumor xenograft: initial study. Q J Nucl Med Mol Imaging 2020.

193. Sachpekidis C, Thieke C, Askoxylakis V, et al. Combined use of (18)F-FDG and (18)F-FMISO in unresectable non-small cell lung cancer patients planned for radiotherapy: a dynamic PET/CT study. Am J Nucl Med Mol Imaging 2015;5(2):127–42. [PubMed: 25973334]

194. Segard T, Robins PD, Yusoff IF, et al. Detection of hypoxia with 18F-fluoromisonidazole (18F-FMISO) PET/CT in suspected or proven pancreatic cancer. Clin Nucl Med 2013;38(1):1–6. [PubMed: 23242037]

195. Pell VR, Baark F, Mota F, et al. PET imaging of cardiac hypoxia: hitting hypoxia where it hurts. Curr Cardiovasc Imaging Rep 2018;11(3):7. [PubMed: 29515752]

196. Imaizumi A, Obata T, Kershaw J, et al. Imaging of hypoxic tumor: correlation between diffusion-weighted MR imaging and (18)F-fluoroazomycin arabinoside positron emission tomography in head and neck carcinoma. Magn Reson Med Sci 2020;19(3):276–81. [PubMed: 31548478]

197. Hamann I, Krys D, Glubrecht D, et al. Expression and function of hexose transporters GLUT1, GLUT2, and GLUT5 in breast cancer-effects of hypoxia. FASEB J 2018;32(9):5104–18. [PubMed: 29913554]

198. Metran-Nascente C, Yeung I, Vines DC, et al. Measurement of tumor hypoxia in patients with advanced pancreatic cancer based on 18F-fluoroazomyin arabinoside uptake. J Nucl Med 2016;57(3):361–6. [PubMed: 26769863]

199. Ventura M, Bernards N, De Souza R, et al. Longitudinal PET imaging to monitor treatment efficacy by liposomal irinotecan in orthotopic patient-derived pancreatic tumor models of high and low hypoxia. Mol Imaging Biol 2020;22(3):653–64. [PubMed: 31482415]

200. Chang E, Liu H, Unterschemmann K, et al. 18F-FAZA PET imaging response tracks the reoxygenation of tumors in mice upon treatment with the mitochondrial complex I inhibitor BAY 87–2243. Clin Cancer Res 2015;21(2):335–46. [PubMed: 25381339]

201. Havelund BM, Holdgaard PC, Rafaelsen SR, et al. Tumour hypoxia imaging with 18F-fluoroazomycinarabinofuranoside PET/CT in patients with locally advanced rectal cancer. Nucl Med Commun 2013;34(2):155–61. [PubMed: 23196674]

202. Capitanio U, Pepe G, Incerti E, et al. The role of 18F-FAZA PET/CT in detecting lymph node metastases in renal cell carcinoma patients: a prospective pilot trial. Eur J Nucl Med Mol Imaging 2020.

203. Pérès EA, Toutain J, Paty LP, et al. 64)Cu-ATSM/(64)Cu-Cl(2) and their relationship to hypoxia in glioblastoma: a preclinical study. EJNMMI Res 2019;9(1):114. [PubMed: 31858290]

204. Pasquali M, Martini P, Shahi A, et al. Copper-64 based radiopharmaceuticals for brain tumors and hypoxia imaging. Q J Nucl Med Mol Imaging 2020.

205. Vāvere AL, Lewis JS. Examining the relationship between Cu-ATSM hypoxia selectivity and fatty acid synthase expression in human prostate cancer cell lines. Nucl Med Biol 2008;35(3):273–9. [PubMed: 18355682]

206. Baark F, Shaughnessy F, Pell VR, et al. Tissue acidosis does not mediate the hypoxia selectivity of [(64)Cu][Cu(ATSM)] in the isolated perfused rat heart. Sci Rep 2019;9(1):499. [PubMed: 30679497]

207. Leung K l-[methyl-(11)C]Methionine. In: Molecular imaging and contrast agent database (MICAD). Bethesda (MD): National Center for Biotechnology Information (US); 2004.

208. Hasebe M, Yoshikawa K, Nishii R, et al. Usefulness of (11)C-methionine-PET for predicting the efficacy of carbon ion radiation therapy for head and neck mucosal malignant melanoma. Int J Oral Maxillofac Surg 2017;46(10):1220–8. [PubMed: 28535963]

209. Zhao J, Chen Z, Cai L, et al. Quantitative volumetric analysis of primary glioblastoma multiforme on MRI and 11C-methionine PET: initial study on five patients. Neurol Neurochir Pol 2019;53(3):199–204. [PubMed: 30855705]

210. Zaragori T, Castello A, Guedj E, et al. Photopenic defects in gliomas with amino-acid PET and relative prognostic value: a multicentric 11C-methionine and 18F-FDOPA PET experience. Clin Nucl Med 2020.

211. Shiiba M, Ishihara K, Kimura G, et al. Evaluation of primary prostate cancer using 11C-methionine-PET/CT and 18F-FDG-PET/CT. Ann Nucl Med 2012;26(2):138–45. [PubMed: 22069194]

212. Lapa C, Garcia-Velloso MJ, Lückerath K, et al. (11) C-Methionine-PET in multiple myeloma: a combined study from two different institutions. Theranostics 2017;7(11):2956–64. [PubMed: 28824728]

213. Drake LR, Hillmer AT, Cai Z. Approaches to PET imaging of glioblastoma. Molecules 2020;25(3).

214. Ceccon G, Lohmann P, Werner JM, et al. Early treatment response assessment using (18)F-FET PET compared to contrast-enhanced MRI in glioma patients following adjuvant temozolomide chemotherapy. J Nucl Med 2020.

215. Kumar M, Salem K, Jeffery JJ, et al. Longitudinal molecular imaging of progesterone receptor reveals early differential response to endocrine therapy in breast cancer with an activating ESR1 mutation. J Nucl Med 2020.

216. Grabher BJ. Breast cancer: evaluating tumor estrogen receptor status with molecular imaging to increase response to therapy and improve patient outcomes. J Nucl Med Technol 2020;48(3):191–201. [PubMed: 32111662]

217. Sipos D, Tóth Z, Lukács G, et al. [F-DOPA PET/MR based target definiton in the 3D based radiotherapy treatment of glioblastoma multiforme patients. First Hungarian experiences]. IdeggyogySz 2019;72(5–6):209–15.

218. Kuten J, Linevitz A, Lerman H, et al. [18F] FDOPA PET may confirm the clinical diagnosis of Parkinson's disease by imaging the nigro-striatal pathway and the sympathetic cardiac innervation: proof-of-concept study. J Integr Neurosci 2020;19(3):489–94. [PubMed: 33070528]

219. Avram M, Brandl F, Cabello J, et al. Reduced striatal dopamine synthesis capacity in patients with schizophrenia during remission of positive symptoms. Brain 2019;142(6):1813–26. [PubMed: 31135051]

220. Gong K, Han PK, Johnson KA, et al. Attenuation correction using deep Learning and integrated UTE/multi-echo Dixon sequence: evaluation in amyloid and tau PET imaging. Eur J Nucl Med Mol Imaging 2020.

221. Shirvan J, Clement N, Ye R, et al. Neuropathologic correlates of amyloid and dopamine transporter imaging in Lewy body disease. Neurology 2019; 93(5):e476–84. [PubMed: 31243072]

222. Schultz AP, Kloet RW, Sohrabi HR, et al. Amyloid imaging of Dutch-type hereditary cerebral amyloid angiopathy carriers. Ann Neurol 2019;86(4):616–25. [PubMed: 31361916]

223. Kero T, Sörensen J, Antoni G, et al. Quantification of (11)C-PIB kinetics in cardiac amyloidosis. J Nucl Cardiol 2020;27(3):774–84. [PubMed: 30039218]

224. Teipel SJ, Temp AGM, Levin F, et al. Association of PET-based stages of amyloid deposition with neuropathological markers of Aβ pathology. Ann Clin Transl Neurol 2020.

225. Palermo G, Tommasini L, Aghakhanyan G, et al. Clinical correlates of cerebral amyloid deposition in Parkinson's disease dementia: evidence from a PET study. J Alzheimers Dis 2019;70(2):597–609. [PubMed: 31256138]

226. Leuzy A, Heurling K, De Santi S, et al. Validation of a spatial normalization method using a principal component derived adaptive template for [(18)F] florbetaben PET. Am J Nucl Med Mol Imaging 2020;10(4):161–7. [PubMed: 32929394]

227. Na S, Jeong H, Park JS, et al. The impact of amyloid-beta positivity with 18F-Florbetaben PET on neuropsychological aspects in Parkinson's disease dementia. Metabolites 2020;10(10).

228. Cho SH, Choe YS, Kim YJ, et al. Concordance in detecting amyloid positivity between (18)F-florbetaben and (18)F-flutemetamol amyloid PET using quantitative and qualitative assessments. Sci Rep 2020;10(1):19576. [PubMed: 33177593]

229. Hellberg S, Silvola JMU, Liljenbäck H, et al. Amyloid-targeting PET Tracer [(18)F]Flutemetamol accumulates in atherosclerotic plaques. Molecules 2019;24(6).

230. Grimmer T, Shi K, Diehl-Schmid J, et al. (18)F-FIBT may expand PET for β-amyloid imaging in neurodegenerative diseases. Mol Psychiatry 2020; 25(10):2608–19. [PubMed: 30120417]

231. Yousefi BH, von Reutern B, Scherübl D, et al. FIBT versus florbetaben and PiB: a preclinical comparison study with amyloid-PET in transgenic mice. EJNMMI Res 2015;5:20. [PubMed: 25918674]

232. Bensaïdane MR, Beauregard JM, Poulin S, et al. Clinical utility of amyloid PET imaging in the differential diagnosis of atypical dementias and its impact on caregivers. J Alzheimers Dis 2016; 52(4):1251–62. [PubMed: 27104896]

233. Rowe CC, Jones G, Doré V, et al. Standardized expression of 18F-NAV4694 and 11C-PiB β-amyloid PET results with the centiloid scale. J Nucl Med 2016;57(8):1233–7. [PubMed: 26912446]

234. Lerdsirisuk P, Harada R, Hayakawa Y, et al. Synthesis and evaluation of 2-pyrrolopyridinylquinoline derivatives as selective tau PET tracers for the diagnosis of Alzheimer's disease. Nucl Med Biol 2020;93:11–8. [PubMed: 33221641]

235. Schönecker S, Brendel M, Palleis C, et al. PET imaging of astrogliosis and tau facilitates diagnosis of Parkinsonian syndromes. Front Aging Neurosci 2019;11:249. [PubMed: 31572166]

236. Malpetti M, Kievit RA, Passamonti L, et al. Microglial activation and tau burden predict cognitive decline in Alzheimer's disease. Brain 2020;143(5):1588–602. [PubMed: 32380523]

237. Nedelska Z, Josephs KA, Graff-Radford J, et al. (18) F-AV-1451 uptake differs between dementia with lewy bodies and posterior cortical atrophy. Mov Disord 2019;34(3):344–52. [PubMed: 30615804]

238. Takenoshita N, Fukasawa R, Ogawa Y, et al. Amyloid and tau positron emission tomography in suggested diabetesrelated dementia. Curr Alzheimer Res 2018;15(11):1062–9. [PubMed: 29984653]

239. Perez-Soriano A, Arena JE, Dinelle K, et al. PBB3 imaging in Parkinsonian disorders: evidence for binding to tau and other proteins. Mov Disord 2017;32(7):1016–24. [PubMed: 28568506]

240. Salinas C, Lohith TG, Purohit A, et al. Test-retest characteristic of [(18)F]MK-6240 quantitative outcomes in cognitively normal adults and subjects with Alzheimer's disease. J Cereb Blood Flow Metab 2020;40(11):2179–87. [PubMed: 31711342]

241. Kuwabara H, Comley RA, Borroni E, et al. Evaluation of 18F-RO-948 (18F-RO6958948) for quantitative assessment of tau accumulation in the human brain with positron emission tomography. J Nucl Med 2018.

242. Honer M, Gobbi L, Knust H, et al. Preclinical evaluation of (18)F-RO6958948, (11)C-RO6931643, and (11)C-RO6924963 as novel PET radiotracers for imaging tau aggregates in Alzheimer disease. J Nucl Med 2018;59(4):675–81. [PubMed: 28970331]

243. Hong CM, Ryu HS, Ahn BC. Early perfusion and dopamine transporter imaging using (18)F-FP-CIT PET/CT in patients with parkinsonism. Am J Nucl Med Mol Imaging 2018;8(6):360–72. [PubMed: 30697456]

244. Suh M, Im JH, Choi H, et al. Unsupervised clustering of dopamine transporter PET imaging discovers heterogeneity of parkinsonism. Hum Brain Mapp 2020;41(16):4744–52. [PubMed: 32757250]

245. Yang Y, Cheon M, Kwak YT. 18F-FP-CIT positron emission tomography for correlating motor and cognitive symptoms of Parkinson's disease. Dement Neurocogn Disord 2017;16(3):57–63. [PubMed: 30906372]

246. Brumberg J, Kerstens V, Cselényi Z, et al. Simplified quantification of [18F]FE-PE2I PET in Parkinson's disease: discriminative power, test–retest reliability and longitudinal validity

during early peak and late pseudo-equilibrium. J Cereb Blood Flow Metab 2021;41(6):1291–300. [PubMed: 32955955]

247. Schmitz TW, Mur M, Aghourian M, et al. Longitudinal Alzheimer's degeneration reflects the spatial topography of cholinergic basal forebrain projections. Cell Rep 2018;24(1):38–46. [PubMed: 29972789]
248. Cyr M, Parent MJ, Mechawar N, et al. PET imaging with [^{1}F]fluoroethoxybenzovesamicol ([^{1}F]FEOBV) following selective lesion of cholinergic pedunculopontine tegmental neurons in rat. Nucl Med Biol 2014;41(1):96–101. [PubMed: 24267056]
249. Bevan-Jones WR, Cope TE, Jones PS, et al. Neuroinflammation and protein aggregation co-localize across the frontotemporal dementia spectrum. Brain 2020;143(3):1010–26. [PubMed: 32179883]
250. Herholz K Cognitive dysfunction and emotionalbehavioural changes in MS: the potential of positron emission tomography. J Neurol Sci 2006; 245(1–2):9–13. [PubMed: 16626746]
251. Kumata K, Zhang Y, Fujinaga M, et al. [(18)F] DAA1106: automated radiosynthesis using spirocyclic iodonium ylide and preclinical evaluation for positron emission tomography imaging of translocator protein (18 kDa). Bioorg Med Chem 2018; 26(17):4817–22. [PubMed: 30166255]
252. Yasuno F, Kosaka J, Ota M, et al. Increased binding of peripheral benzodiazepine receptor in mild cognitive impairment-dementia converters measured by positron emission tomography with [^{11}C]DAA1106. Psychiatry Res 2012;203(1):67–74. [PubMed: 22892349]
253. Fan Z, Dani M, Femminella GD, et al. Parametric mapping using spectral analysis for (11)C-PBR28 PET reveals neuroinflammation in mild cognitive impairment subjects. Eur J Nucl Med Mol Imaging 2018;45(8):1432–41. [PubMed: 29523926]
254. Varnäs K, Cselényi Z, Jucaite A, et al. PET imaging of [(11)C]PBR28 in Parkinson's disease patients does not indicate increased binding to TSPO despite reduced dopamine transporter binding. Eur J Nucl Med Mol Imaging 2019; 46(2):367–75. [PubMed: 30270409]
255. Herranz E, Louapre C, Treaba CA, et al. Profiles of cortical inflammation in multiple sclerosis by (11)C-PBR28 MR-PET and 7 Tesla imaging. Mult Scler 2020;26(12):1497–509. [PubMed: 31368404]
256. Tran TT, Gallezot JD, Jilaveanu LB, et al. [(11)C] Methionine and [(11)C]PBR28 as PET imaging tracers to differentiate metastatic tumor recurrence or radiation necrosis. Mol Imaging 2020;19. 1536012120968669.
257. Mabrouk R, Strafella AP, Knezevic D, et al. Feasibility study of TSPO quantification with [18F]FEPPA using population-based input function. PLoS One 2017;12(5):e0177785. [PubMed: 28545084]
258. Yilmaz R, Strafella AP, Bernard A, et al. Serum inflammatory profile for the discrimination of clinical subtypes in Parkinson's disease. Front Neurol 2018;9:1123. [PubMed: 30622507]
259. Leung K N-Acetyl-N-(2-[(18)F]fluoroethoxybenzyl)-2-phenoxy-5-pyridinamine. In: Molecular imaging and contrast agent database (MICAD). Bethesda (MD): National Center for Biotechnology Information (US); 2004.
260. Vasdev N, Green DE, Vines DC, et al. Positron-emission tomography imaging of the TSPO with [(18)F]FEPPA in a preclinical breast cancer model. Cancer Biother Radiopharm 2013;28(3):254–9. [PubMed: 23350894]
261. James ML, Belichenko NP, Nguyen TV, et al. PET imaging of translocator protein (18 kDa) in a mouse model of Alzheimer's disease using N-(2,5-dimethoxybenzyl)-2–18F-fluoro-N-(2-phenoxyphenyl) acetamide. J Nucl Med 2015;56(2):311–6. [PubMed: 25613536]
262. Singhal T, Rissanen E, Ficke J, et al. Widespread glial activation in primary progressive multiple sclerosis revealed by 18F-PBR06 PET: a clinically feasible, individualized approach. Clin Nucl Med 2020.
263. Singhal T, O'Connor K, Dubey S, et al. 18F-PBR06 versus 11C-PBR28 PET for assessing white matter translocator protein binding in multiple sclerosis. Clin Nucl Med 2018;43(9):e289–95. [PubMed: 30004939]
264. Zhang H, Tan H, Mao W-J, et al. 18F-PBR06 PET/CT imaging of inflammation and differentiation of lung cancer in mice. Nucl Sci Tech 2019;30(5):83.

265. Edison P, Donat CK, Sastre M. In vivo imaging of glial activation in Alzheimer's disease. Front Neurol 2018;9:625. [PubMed: 30131755]
266. Dupont AC, Largeau B, Santiago Ribeiro MJ, et al. Translocator protein-18 kDa (TSPO) positron emission tomography (PET) imaging and its clinical impact in neurodegenerative diseases. Int J Mol Sci 2017;18(4).
267. Datta G, Colasanti A, Kalk N, et al. (11)C-PBR28 and (18)F-PBR111 detect white matter inflammatory heterogeneity in multiple sclerosis. J Nucl Med 2017;58(9):1477–82. [PubMed: 28302760]
268. Ottoy J, De Picker L, Verhaeghe J, et al. (18)F-PBR111 PET imaging in healthy controls and schizophrenia: test-retest reproducibility and quantification of neuroinflammation. J Nucl Med 2018; 59(8):1267–74. [PubMed: 29326362]
269. Hu W, Pan D, Wang Y, et al. PET imaging for dynamically monitoring neuroinflammation in APP/PS1 mouse model using [(18)F]DPA714. Front Neurosci 2020;14:810. [PubMed: 33132817]
270. Van Weehaeghe D, Babu S, De Vocht J, et al. Moving toward multicenter therapeutic trials in amyotrophic lateral sclerosis: feasibility of data pooling using different translocator protein PET radioligands. J Nucl Med 2020;61(11):1621–7. [PubMed: 32169920]
271. Bahri MA, Plenevaux A, Aerts J, et al. Measuring brain synaptic vesicle protein 2A with positron emission tomography and [18F]UCB-H. Alzheimers Dement (N Y) 2017;3(4):481–6. [PubMed: 29124105]
272. Serrano ME, Becker G, Bahri MA, et al. Evaluating the in vivo specificity of [(18)F]UCB-H for the SV2A protein, compared with SV2B and SV2C in rats using microPET. Molecules 2019;24(9).
273. Estrada S, Lubberink M, Thibblin A, et al. [(11)C] UCB-A, a novel PET tracer for synaptic vesicle protein 2A. Nucl Med Biol 2016;43(6):325–32. [PubMed: 27260773]
274. Rokka J, Schlein E, Eriksson J. Improved synthesis of SV2A targeting radiotracer [11C]UCB-J. EJNMMI Radiopharm Chem 2019;4(1):30. [PubMed: 31784919]
275. Cai Z, Li S, Zhang W, et al. Synthesis and preclinical evaluation of an 18F-labeled synaptic vesicle glycoprotein 2A PET imaging probe: [18F]SynVesT-2. ACS Chem Neurosci 2020;11(4):592–603. [PubMed: 31961649]
276. Naganawa M, Li S, Nabulsi NB, et al. First-in-human evaluation of (18)F-SynVesT-1, a novel radioligand for PET imaging of synaptic vesicle protein 2A. J Nucl Med 2020.
277. Papadakis GZ, Kochiadakis G, Lazopoulos G, et al. Targeting vulnerable atherosclerotic plaque via PET-tracers aiming at cell-surface overexpression of somatostatin receptors. Biomed Rep 2020;13(3):9. [PubMed: 32765848]
278. Vachatimanont S, Kunawudhi A, Promteangtrong C, et al. Benefits of [(68)Ga]-DOTATATE PET-CT comparable to [(18)F]-FDG in patient with suspected cardiac sarcoidosis. J Nucl Cardiol 2020.
279. Lee H, Eads JR, Pryma DA. 68) Ga-DOTATATE positron emission tomography-computed tomography quantification predicts response to somatostatin analog therapy in gastroenteropancreatic neuroendocrine tumors. Oncologist 2020.
280. Guirguis MS, Adrada BE, Surasi DS, et al. 68Ga-DOTATATE uptake in primary breast cancer. Clin Nucl Med 2020.

KEY POINTS

- New radiopharmaceuticals can enable imaging strategies for the better understanding of disease states in oncology, neurology, and cardiovascular disease.
- Oncologic PET imaging agents are intended to probe the biological characteristics of cancers to improve diagnostics and the efficacy of therapeutic strategies.
- Nononcology neurologic PET imaging focuses on a range of neurologic disorders with an emphasis placed on neurodegenerative diseases such as Parkinson disease and Alzheimer disease.
- Most cardiac PET imaging has focused on blood flow and metabolism and is complemented by additional compounds for imaging of atherosclerosis.

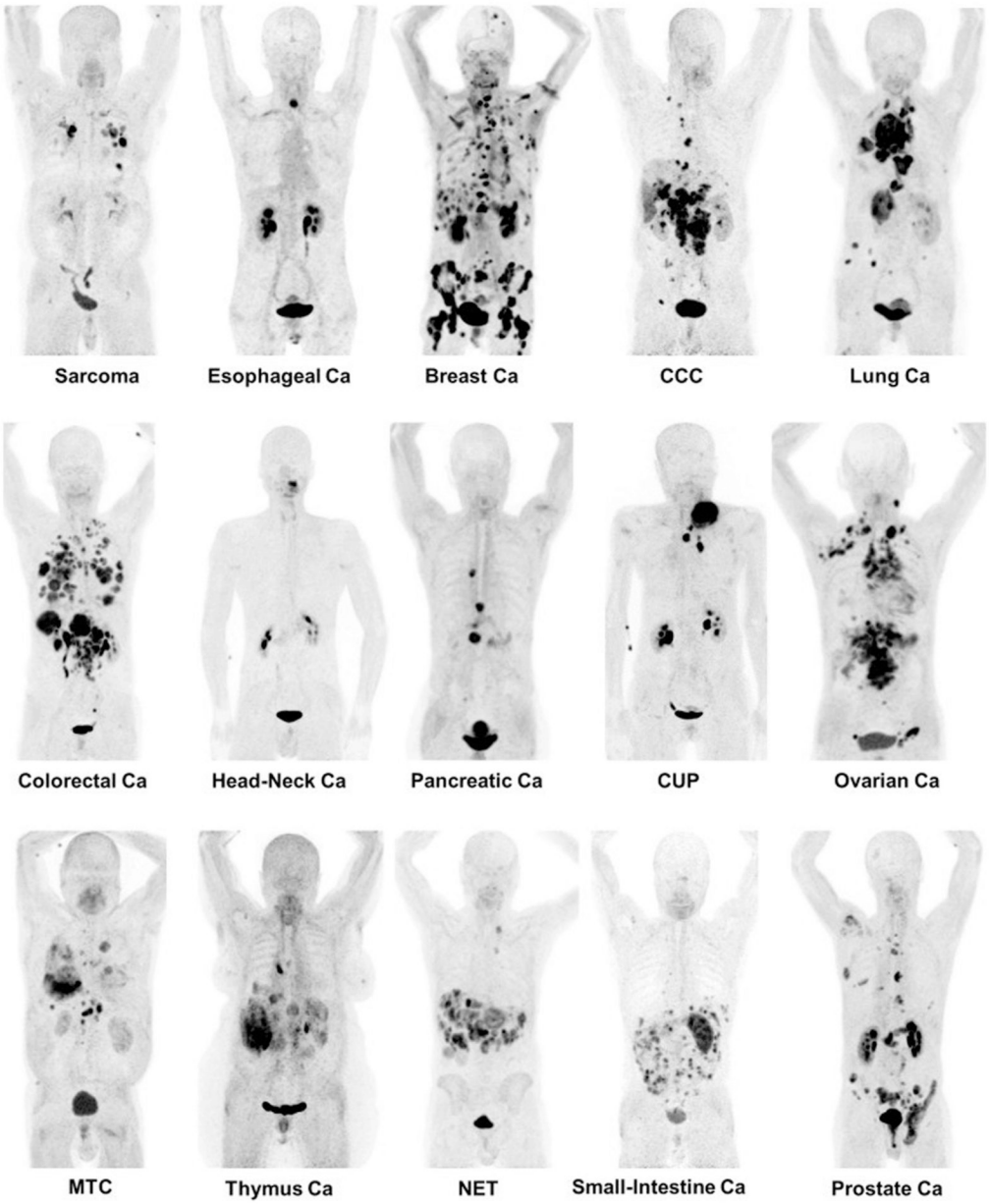

Fig. 1.

[^{68}Ga] fibroblast-activating protein inhibitor-4 imaging in multiple types of cancer. Ca, cancer; CCC, circulating cancer cell; CUP, cancer of unknown primary; MTC, medullary thyroid cancer; NET, neuroendocrine tumor. (*From* Kratochwil C, Flechsig P, Lindner T, et al. (68)Ga-FAPI PET/CT: Tracer Uptake in 28 Different Kinds of Cancer. *J Nucl Med.* 2019;60(6):801–805.)

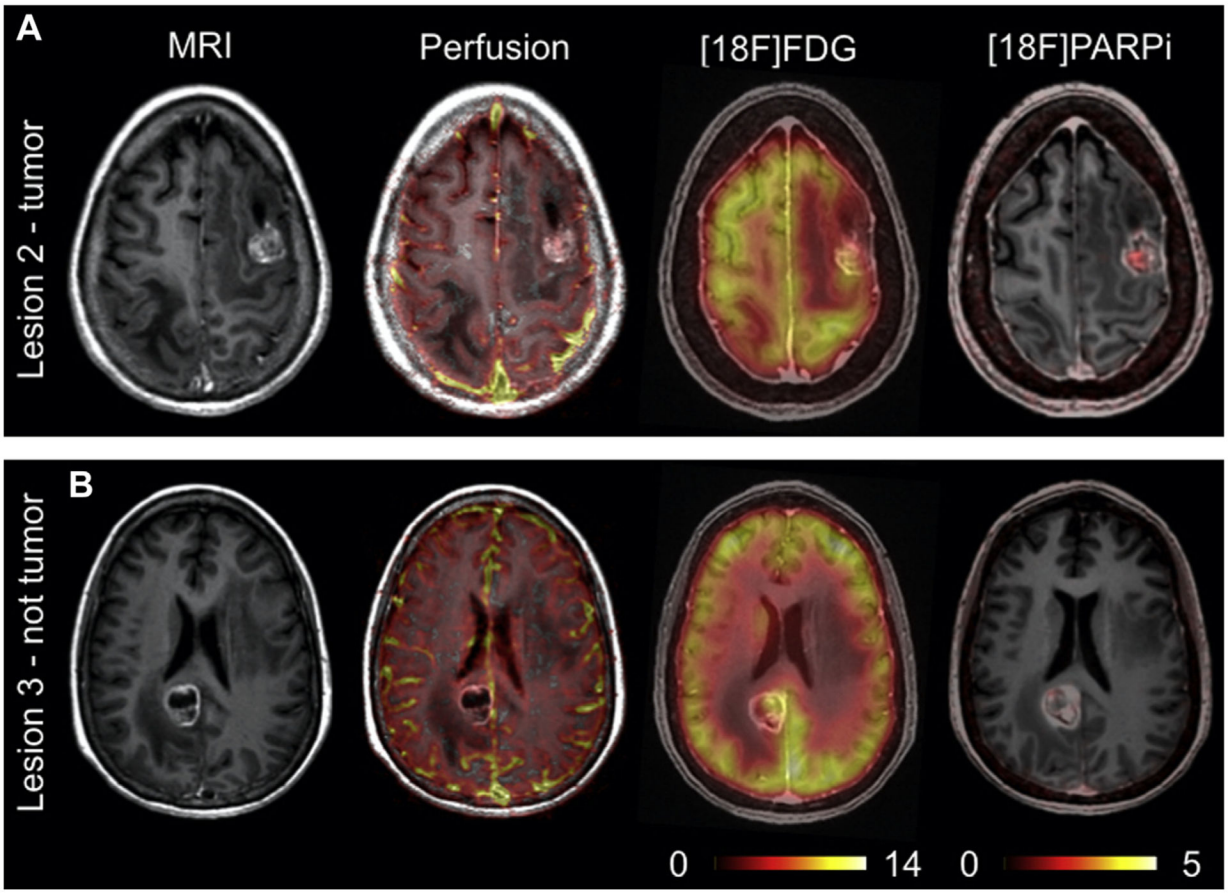

Fig. 2.

[^{18}F]F-PARPi imaging in a patient with benign and malignant lesions within the brain. (*A*) Lesion from patient confirmed to be cancerous (*B*) Lesion from patient confirmed to be non-cancerous. (*From* Young RJ, Demétrio De Souza França P, Pirovano G, et al. Preclinical and first-in-human-brain-cancer applications of [18F]poly-(ADP-ribose) polymerase inhibitor PET/MR. *Neuro-Oncology Advances*. 2020.)

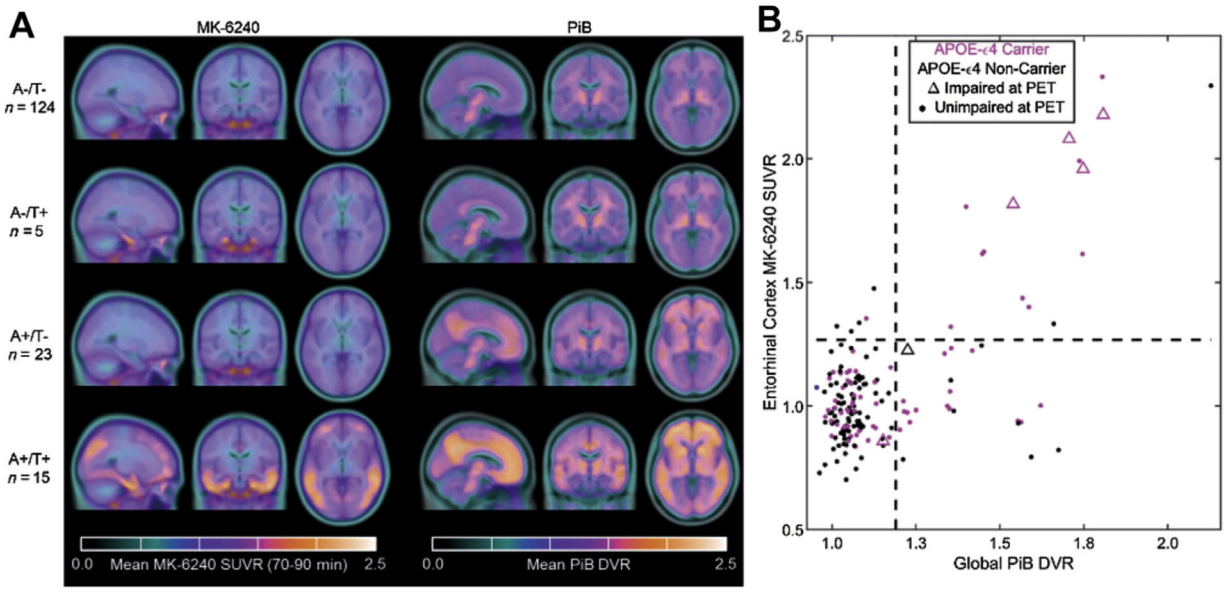

Fig. 3.

MK-6240 and PiB PET/CT images, and biomarker group stratification. (*A*) PET/CT images of the [11C]PiB and [18F]MK6240 tracers in different patient groups. (*B*) Quantrant plots representing the relationship between global PiB distribution volume ratio (DVR) and MK6240 standard uptake value ratio (SUVR) in entorhinal cortex. Results suggest that changes in PiB precede detectable changes in MK-6240 in most cases. Individuals with mild cognitive impairment at PET (*triangles*) were more likely to be both amyloid (A) and tau (T) positive than any other group. (*From* Betthauser TJ, Koscik RL, Jonaitis EM, et al. Amyloid and tau imaging biomarkers explain cognitive decline from late middle-age. *Brain*. Jan 1 2020;143(1):320–335. https://doi.org/10.1093/brain/awz378.)

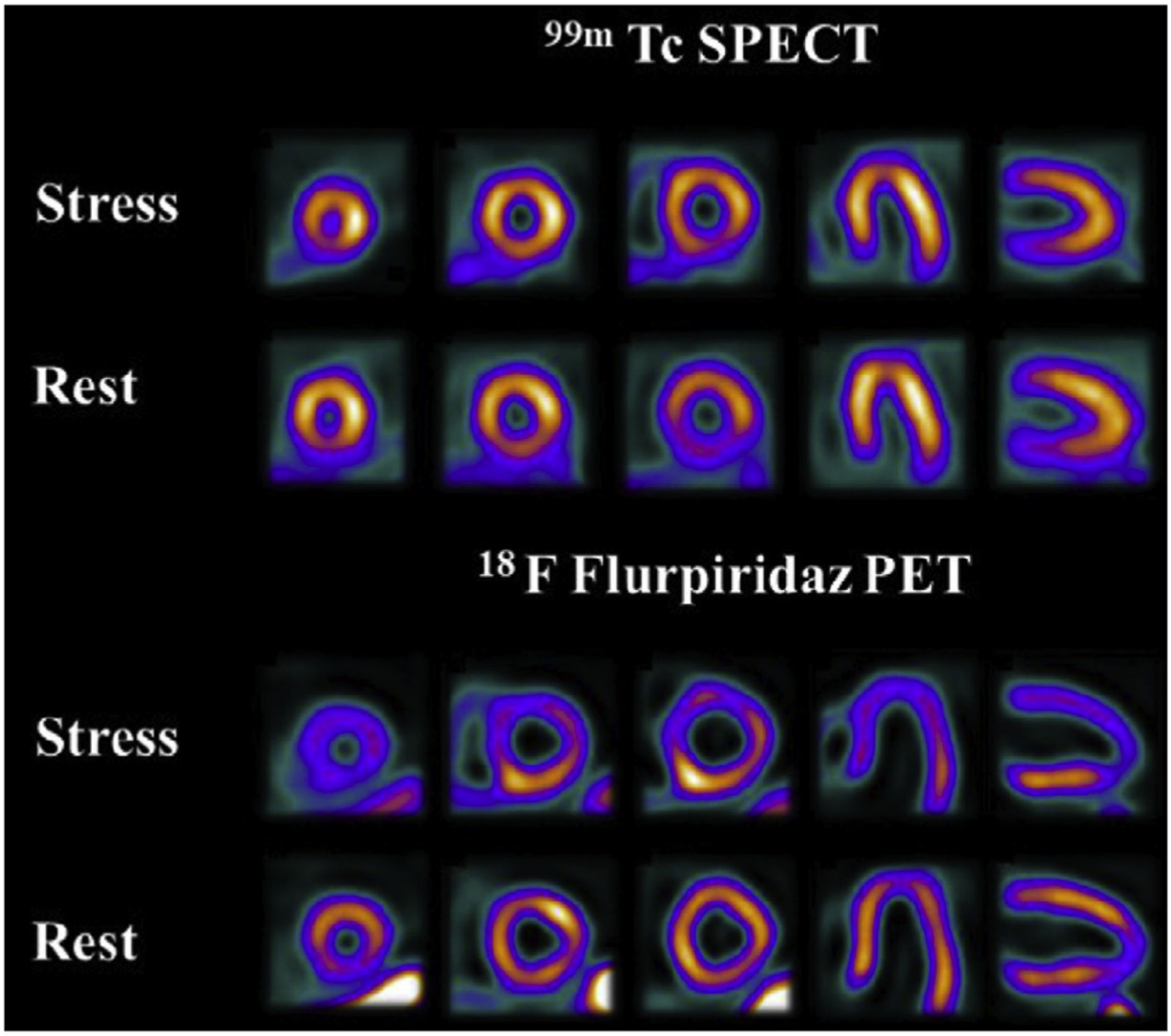

Fig. 4.

Rest and pharmacological stress SPECT and [^{18}F]flurpiridaz PET images. This 82-year-old male patient without a history of myocardial infarction had 100% proximal obtuse marginal occlusion as well as 56% proximal and 80% distal left circumflex stenoses. Both studies are true-positive, but stress and rest perfusion defects in the lateral wall are more prominent and larger on PET than on SPECT images. (*From* Maddahi J, Lazewatsky J, Udelson JE, et al. Phase-III Clinical Trial of Fluorine-18 Flurpiridaz Positron Emission Tomography for Evaluation of Coronary Artery Disease. *Journal of the American College of Cardiology*. 2020/07/28/ 2020;76(4):391–401.)

Table 1

Prominent and novel tracers and their current status

Imaging Agent	Clinical Application	Biological Target	Current Status	Example Clinical Trials
[^{68}Ga]Ga-FAPI	Oncology;[4] Head and neck cancer[168] Esophageal cancer Breast cancer Metastatic Breast cancer[9] Sarcoma Lung cancer[169] Colorectal cancer[170] Pancreatic cancer[171] Prostate cancer[172] Ovarian cancer Cardiology; myocardial infarction[173]	Fibroblast activation protein expressed on fibroblasts	Phase I/II clinical trials	NCT04588064, NCT04457258, NCT04504110, NCT04147494, NCT04441606, NCT04457232, NCT04459273, NCT04571086, NCT04499365, NCT04554719, NCT04416165, NCT04367948
[^{18}F]F-FLT	Oncology; Glioblastoma multiforme[174] Head and neck cancer[22] Breast cancer[175] Metastatic Breast cancer[176] Small cell lung cancer[177] Non–small cell lung cancer[178] Lymphoma[18,25,180] Sarcoma[19]	Internalized and phosphorylated by proliferating cells	Phase II/III clinical trials	NCT03318497, NCT04221438, NCT04271436, NCT01244737, NCT02392429, NCT03276676, NCT04037462
[^{68}Ga]Ga-PSMA	Oncology: Glioblastoma[179] Breast cancer[35,37] Metastatic Breast cancer[37] Triple-negative breast cancer[180] Prostate cancer[29,31,33]	PSMA expression	Phase II/III clinical trials	NCT04614363, NCT03689582, NCT03903419, NCT04147494, NCT04402151
[^{89}Zr]Zr-SC16	Oncology; Small cell lung cancer[38,41] Neuroendocrine prostate cancer[181,182]	DLL3 expression	Preclinical: Phase I clinical trials	NCT04199741
[^{18}F]F-PARPi	Oncology: Head and neck cancer[51] Brain cancer[183,184] Prostate cancer[50]	PARP1 enzyme in nucleus	Preclinical: Phase I clinical trials	NCT04173104, NCT03631017
[^{18}F]F-FluorThanatrace	Oncology: Glioblastoma Breast cancer[185] Pancreatic cancer[49] Ovarian cancer Prostate cancer	PARP1 enzyme in nucleus	Preclinical: Phase I clinical trials	NCT03492164, NCT03334500, NCT04221061, NCT03604315, NCT03083288

Imaging Agent	Clinical Application	Biological Target	Current Status	Example Clinical Trials
[^{89}Zr]Zr-pembrolizumab	Oncology:[64,65] Non–small cell lung cancer Melanoma	PD-1 expression	Preclinical: Phase I/II clinical trials	NCT02760225, NCT03065764
[^{89}Zr]Zr-ipilimumab	Oncology:[186] Metastatic melanoma	CTLA-4 expression	Preclinical: Phase I clinical trials	NCT03313323
[^{89}Zr]Zr-atezolizumab	Oncology:[187] Metastatic breast cancer Rectal cancer Diffuse large B-cell lymphoma	PD-L1 expression	Preclinical: Phase I clinical trials	NCT04222426, NCT03850028, NCT04564482
[^{89}Zr]Zr-avelumab	Oncology: Breast cancer[188,189] Non–small cell lung cancer	PD-L1 expression	Preclinical: Phase I clinical trials	NCT03514719
[^{18}F]F-AraG	Oncology: Head and neck cancers Triple-negative breast cancer Non–small cell lung cancer Rhabdomyosarcoma[68]	Activated T cells	Preclinical: Phase I clinical trials	NCT04052412, NCT03071757
[^{18}F]F-pHLIP	Oncology: Breast cancer[73] Prostate cancer[190]	Acidic conditions of interstitial space in tumors	Preclinical: Phase I clinical trials	NCT04054986
[^{18}F]FMISO	Oncology: Head and neck cancer[191] brain cancer Breast cancer[192] Non–small cell lung cancer[193] Pancreatic adenocarcinoma[194] Sarcoma Cardiology: Cardiac ischemia[195]	Hypoxic conditions within tumor microenvironment	Preclinical: Phase I/II clinical trials	NCT02016872, NCT03730077, NCT01967927, NCT03649880, NCT00606294, NCT03865277, NCT04309552, NCT02498613, NCT01507428
[^{18}F]F-FAZA	Oncology: Head and neck cancer[196] Glioma[82] Neuroendocrine cancer Breast cancer[197] Lung cancer[80] Pancreatic cancer[198,199] Cervical cancer Prostate cancer[200] Colorectal cancer[201] Renal cell carcinoma[202] Sarcoma Rhabdomyosarcoma	Hypoxic conditions within tumor microenvironment	Preclinical: Phase I/II clinical trials	NCT03955393, NCT02701699, NCT01542177, NCT03054792, NCT01567800, NCT03168737, NCT04395469, NCT01549730, NCT02394652, NCT03513042
[^{64}Cu]Cu-ATSM	Oncology: Glioblastoma[203,204] Prostate cancer[205] Rectal cancer Cardiology: Cardiac ischemia[206]	Hypoxic conditions within tumor microenvironment	Preclinical: Phase I clinical trials	NCT03951337

Imaging Agent	Clinical Application	Biological Target	Current Status	Example Clinical Trials
[^{11}C]C-MET	Oncology:[207] Head and neck cancer[208] Glioblastoma[209] Glioma[210] Breast cancer[207] Mesothelioma Prostate cancer[211] Multiple myeloma[212] Melanoma	Increased amino acid transport and protein incorporation in cancer cells	Preclinical: Phase I/II clinical trials	NCT03977896, NCT03739333, NCT03009318, NCT00840047, NCT00002981, NCT02519049
[^{18}F]F-FET	Oncology: Glioblastoma multiforme[213] Glioma[214] Brain neoplasms[90]	LAT-1–based amino acid transport	Preclinical: Phase I/II clinical trials	NCT01756352, NCT03402425, NCT01756352, NCT04001257, NCT04044937,
[^{18}F]F-FES	Oncology: Breast cancer[215,216] Metastatic breast cancer	Estrogen receptor expression	Preclinical: Phase I/II/III clinical trials	NCT03544762, NCT03703492, NCT02409316, NCT01986569, NCT04150731
[^{18}F]F-FFNP	Oncology: Breast cancer[93]	Progesterone receptor expression	Preclinical: Phase I/II clinical trials	NCT03212170, NCT02455453, NCT00968409, NCT03212170
[^{18}F]FDOPA	Oncology: Glioblastoma[217] Glioma[88] Neurology: Parkinson disease[218] Schizophrenia[219]	LAT-1 expression in amino acid transport and aromatic acid decarboxylase–mediated conversion to dopamine	Preclinical: Phase I/II clinical trials	NCT03903419, NCT03778294, NCT02104310, NCT03042416 NCT03648905, NCT04459052, NCT04038957
[^{11}C]C-PiB	Neurology: Alzheimer disease[220] Parkinson disease[221] Dementia Cerebral amyloid angiopathy[222] Cardiology: Cardiac amyloidosis[223]	Amyloid-β plaques	Preclinical: Phase I/II/III clinical trials	NCT03555292, NCT03981380, NCT03958630, NCT03172117, NCT03969732
[^{18}F]F-florbetapir	Neurology: Alzheimer disease[224] Parkinson disease[225] Dementia	Amyloid-β plaques	Preclinical: Phase I/II/III clinical trials	NCT03019029, NCT04305210, NCT04248270, NCT02813434, NCT03282916
[^{18}F]F-florbetaben	Neurology: Alzheimer disease[226] Parkinson disease[227] Dementia Cardiology: Atherosclerosis[160]	Amyloid-β plaques	Preclinical: Phase I/II/III clinical trials	NCT03706261, NCT02831283, NCT04576793, NCT03019536
[^{18}F]F-flutemetamol	Neurology: Alzheimer disease[228] PD Dementia Cardiology: Atherosclerosis[229]	Amyloid-β plaques	Preclinical: Phase I clinical trials	NCT03291093, NCT02685969, NCT03174938, NCT01979419, NCT03466177

Imaging Agent	Clinical Application	Biological Target	Current Status	Example Clinical Trials
[^{18}F]FIBT	Neurology:[230,231] AD PD Dementia	Amyloid-β plaques	Preclinical	—
[^{18}F]NAV4694	Neurology:[232] Alzheimer disease[233] PD Dementia	Amyloid-β plaques	Preclinical: Phase I clinical trials	NCT00838877, NCT00991419, NCT01325402
[^{18}F]F-THK5351	Neurology: Alzheimer disease[234] Parkinson disease[235] Dementia	Tau protein	Preclinical: Phase I/II clinical trials	NCT02686216, NCT04318626, NCT03430869, NCT04588649
[^{18}F]F-AV-1451	Neurology: Alzheimer disease[236] PD Dementia[237]	Tau protein	Preclinical: Phase I/II/III clinical trials	NCT02350634, NCT02958670, NCT03189485, NCT03816228, NCT03143374, NCT00950430, NCT01687153, NCT02854033
[^{11}C]C-PBB3	Neurology: Alzheimer disease[238] Parkinson disease[239] Dementia	Tau protein	Preclinical: Phase I clinical trials	NCT04101968
[^{18}F]F-MK-6240	Neurology: Alzheimer disease[120,240] PD Dementia	Tau protein	Preclinical: Phase I/II clinical trials	NCT03373604, NCT03372317, NCT03706261, NCT04576793, NCT04098666, NCT03053908
[^{18}F]F-Ro-6958948	Neurology: Alzheimer disease[241,242] PD Dementia	Tau protein	Preclinical: Phase I clinical trials	NCT04482660
[^{18}F]F-FP-CIT	Neurology: Alzheimer disease[243] Parkinson disease[244,245] Dementia	Dopamine transporter	Preclinical: Phase I clinical trials	NCT04334902
[^{18}F]F-FE-PE2I	Neurology: Parkinson disease[131,246]	Dopamine transporter	Preclinical: Phase I clinical trials	NCT04243304
[^{18}F]F-FEOBV	Neurology: Alzheimer disease[247] Parkinson disease[248] Dementia	Vesicular acetylcholine transporter	Preclinical: Phase I clinical trials	NCT03554551, NCT04291144, NCT03647137
[^{11}C]C-PK-11195	Neurology:[249] AD PD Multiple sclerosis[250]	Translocator protein	Preclinical: Phase I clinical trials	NCT04239820, NCT03368677, NCT04171882, NCT04126772, NCT03134716

Radiol Clin North Am. Author manuscript; available in PMC 2022 September 01.

Imaging Agent	Clinical Application	Biological Target	Current Status	Example Clinical Trials
[^{11}C]C-DAA1106	Neurology:[251] Alzheimer disease[252]	Translocator protein	Preclinical	
[^{11}C]C-PBR28	Neurology: Alzheimer disease[253] Parkinson disease[254] Multiple sclerosis[255] Oncology:[256] Lung cancer Melanoma	Translocator protein	Preclinical: Phase I/II clinical trials	NCT04230174, NCT02831283, NCT04274998, NCT03787446, NCT02702102
[^{18}F]F-FEPPA	Neurology: Alzheimer disease[257] Parkinson disease[257,258] Multiple sclerosis[259] Major depression disorders Oncology: Breast cancer[260]	Translocator protein	Preclinical: Phase I clinical trials	NCT00970333, NCT02983318
[^{18}F]F-PBR06	Neurology: Alzheimer disease[261] PD Multiple sclerosis[262,263] Oncology: Lung cancer[264]	Translocator protein	Preclinical: Phase I clinical trials	NCT04510220, NCT04144257, NCT03983252, NCT01028209
[^{18}F]F-PBR111	Neurology: Alzheimer disease[265] Parkinson disease[266] Multiple sclerosis[267] Schizophrenia[268]	Translocator protein	Preclinical: Phase I/II clinical trials	NCT01209156, NCT02009826, NCT01428505
[^{18}F]F-DPA714	Neurology: Alzheimer disease[141,269] PD Multiple sclerosis Amyotrophic lateral sclerosis[270]	Translocator protein	Preclinical: Phase I/II clinical trials	NCT03691077, NCT04171882, NCT03230526, NCT02305264
[^{18}F]F-UCB-H	Neurology: Alzheimer disease[271] Epilepsy[272]	SV2A	Preclinical	
[^{11}C]C-UCB-A	Neurology: AD Epilepsy[273]	SV2A	Preclinical	
[^{11}C]C-UCB-J	Neurology: AD PD Multiple Sclerosis Epilepsy[274] Schizophrenia	SV2A	Preclinical: Phase I/II clinical trials	NCT03577262, NCT03493282, NCT04038840, NCT04243304, NCT03134716

Imaging Agent	Clinical Application	Biological Target	Current Status	Example Clinical Trials
[^{18}F]F-SynVesT-1	Neurology:[275] AD PD Multiple sclerosis Epilepsy[276]	SV2A	Preclinical: Phase I clinical trials	NCT04634994
[^{18}F]F-flurpiridaz	Cardiology:[151] Coronary artery disease Ischemic heart disease	Myocardial perfusion imaging	Preclinical: Phase I clinical trials	NCT04594941, NCT03354273
[^{68}Ga]Ga-DOTATATE	Cardiology: Atherosclerosis[277] Cardiac sarcoidosis[278] Oncology: Neuroendocrine tumors[279] Breast cancer[280] Pancreatic cancer Prostate cancer	Somatostatin receptor 2	Preclinical: Phase I/II clinical trials	NCT04043377, NCT04073810, NCT04032197, NCT02840149, NCT03145857, NCT04041882
[^{64}Cu]Cu-DOTA-ECL1i	Cardiology: Atherosclerosis Oncology: Head and neck cancer Pancreatic cancer	Somatostatin receptor 2	Preclinical: Phase I clinical trials	NCT04537403, NCT03851237, NCT04217057

The preclinical and clinical research examples provided in this table are not an exhaustive representation of all the work being performed with these PET tracers.